

## **Characterization of phytoplankton functional groups in a tropical shellfish harvesting estuary (Ashtamudi) and adjacent nearshore waters (southwest coast of India)**

**Peariya Anil, Nikathithara Velappan Madhu \*, Chazhikulam Rajan Vishal, Ponnaratta Gopika, Sukumaran Jyothi, Kanneth Satheesan Arya, Thundiyl Raju Gireeshkumar**

CSIR-National Institute of Oceanography, Regional Centre,

Dr.Salim Ali Road, Kochi-682018, Kerala, India

\*-E mail corresponding author - nmadhu@nio.org

### **Abstract**

A pioneering study on phytoplankton marker pigments, by adopting the HPLC-CHEMTAX analytical approach, was carried out in one of the major shellfish harvesting estuaries (Ashtamudi estuary-AE) on the southwest coast of India and also its adjacent nearshore waters (<20 m depth) to study the dynamics of phytoplankton functional groups (PFGs). The AE, in general, appeared to be warm (>29°C) during the non-monsoon seasons, along with the prevalence of higher salinity (> 25) and NH<sub>4</sub>-N (> 5µM) levels. However, during the summer monsoon (SM), the prevailing substantial river influx converted the AE into a low salinity (<10) dominated system, provided with enhanced levels of NO<sub>3</sub>-N (4.6-12.6 µM) and PO<sub>4</sub>-P (0.2-1.4µM), specifically on its upper reaches. The dissolved inorganic nitrogen (DIN) in the AE was mainly comprised of ammonium (NH<sub>4</sub>-N), approximately up to ~81.8% of the DIN, regardless of seasons, which signifies the eutrophic state of the estuary, the upstream sampling locations, in particular. Concerning the phytoplankton community, a pronounced spatio-temporal variation in chlorophyll *a* biomass was discernible in the AE, with an exceptional increase (6.4 - 12.1 mg m<sup>-3</sup>) during the SIM period. The prevalence of a conspicuous increase in chlorophyll *a* (av. >5 mg m<sup>-3</sup>) along with enhanced zeaxanthin (av. >1.5 mg m<sup>-3</sup>) recorded in the AE during the non-monsoon (specifically SIM period) season apparently signified the characteristic governance of cyanobacterial community. During the SM period, the estuary sustained more or less similar concentrations of certain marker pigments, i.e. alloxanthin, zeaxanthin, fucoxanthin and chl *b*, which representing the co-occurrence of cryptophytes, cyanobacteria, diatoms and chlorophytes, respectively. In contrast, the nearshore waters, wherein enhanced nitrate (NO<sub>3</sub>-N) and phosphate (PO<sub>4</sub>-P) levels prevailed, irrespective of seasons, sustained dominance of fucoxanthin over other marker pigments, which indicated the numerical supremacy of diatoms. The CHEMTAX analysis, adopted for estimating the chlorophyll *a* equivalents of various PFGs, corroborated the supremacy of cyanobacterial derived chlorophyll *a* in the estuary, and it was conspicuous during the non-monsoonal seasonal periods. Even though the estuary has shown remarkable spatio-temporal hydrographic inconsistencies, that variability was not much operative in generating extreme changes in the nutrient components and subsequent phytoplankton community compositions. From the conspicuous increase in N:P and Si:P ratios, resulting mainly from the low levels of P, it can be concluded that the AE has been a P-limited system for phytoplankton growth (especially for large-sized phytoplankton, e.g., diatoms and dinoflagellates), mainly during the non-monsoonal seasonal periods. Perhaps, this P-limitation, along with the prevalence of warm water column and enhanced NH<sub>4</sub>-N levels, could be the potential causes of the preponderance of cyanobacterial populations in the AE.

**Keywords:-** Estuary; Ashtamudi; Phytoplankton; Diatoms; Cyanobacteria; CHEMTAX

## 1. Introduction

Phytoplankton communities in tropical and sub-tropical coastal waters exhibit a remarkable spatio-temporal variation in their biomass (chlorophyll a), productivity and community composition because of the drastic environmental discrepancies (Paerl et al.2010; Cavalcanti et al.2020). These regions are regarded as one of the most productive coastal ecosystems worldwide because of the persistent enhanced nutrient supply (Cloern et al.2014). Normally, estuaries in these geographical regimes are known for their pronounced seasonality in phytoplankton growth (mainly in diatoms) because of the prevailing seasonally shifting nutrient-rich freshwaters and nutrient-poor marine waters (Quinlan and Phlips, 2007; Cavalcanti et al.2020). Classically, phytoplankton community compositional variations in aquatic systems are evaluated by microscopy involving identification, enumeration of cells, measuring their cell size and converting volumes to carbon biomass (Utermöhl, 1958). Nevertheless, this method was considered time-consuming and also required sound taxonomic knowledge to identify phytoplankton genus or species. Eventhough this conventional method is regarded as accurate in identifying phytoplankton species, the precision is low unless many cells are enumerated. Moreover, microscope-based species identification is often experiencing great difficulty in identifying smaller phytoplankton (<2 µm), called picoautotrophs (Jeffrey, 1997), which form the principal primary producers in the oligotrophic open ocean (Agusti et al.2019) as well as in the mesotrophic or eutrophic coastal waters (Gaulke et al.2010). To overcome such analytical constraints, the high performance liquid chromatography (HPLC) technique was implemented few decades ago worldwide which can estimate not only chlorophyll a concentrations more efficiently than fluorometry but also the carotenoid pigments of taxonomic relevance, including the fragile forms of phytoplankton (e.g., nano-pico sized phytoplankton such as cyanobacteria, chlorophytes, cryptophytes, haptophytes, chrysophytes, etc.) that do not withstand common fixative procedures (Mackey et al 1996; Roy et al.2015). Certain marker pigments, mainly fucoxanthin, peridinin, zeaxanthin, alloxanthin, 19'hex-fucoxanthin, 19'but-fucoxanthin and chlorophyll b are considered the biomarkers of major phytoplankton functional groups (PFGs), for example, diatoms, dinoflagellates, cyanobacteria, cryptophytes, haptophytes, chrysophytes and chlorophytes, respectively (Barlow et al.2008). These marker pigments, in general, are used to understand the physiological status of the individual PFG affected by the prevailing environmental changes (Paerl et al. 2003; Roy et al.2006). Furthermore, biomarker-based chemotaxonomic (CHEMTAX) analysis elucidates the chlorophyll a contribution of each PFG to the total phytoplankton biomass, and it has been widely used to characterise phytoplankton composition in different regions of the world ocean (Mackey et al.1996; Wright et al.2010). However, as far as the tropical coastal waters, especially the

estuaries, are concerned, this application is limited by the lack of known pigment ratios (Wright et al. 1996).

The southwest coast of India is endowed with several dynamic estuaries, and most of them are biologically highly productive (Qasim, 2003; Madhu et al.2007; Patil and Anil, 2015). Generally, these estuaries are greatly influenced by the natural and anthropogenic pressures on a spatio-temporal scale (Qasim, 2003). During the southwest monsoon (SWM) or summer monsoon (SM) period, rivers associated with these estuaries carry a huge quantity of terrigenous materials (both autochthonous and allochthonous origin) via the fluvial discharge and, consequently, enable the estuaries into freshwater dominated systems (Qasim, 2003). Constant mixing of freshwaters with the neritic waters because of tidal activity, the hydrographic properties of these estuaries are significantly spatially variable (Sebin et al.2020). Indeed, the SWM-influenced torrential rainfall has a vital role in the temporal variability of hydro-chemical properties of these estuaries (Qasim, 2003). The Ashtamudi estuary (AE hereafter), the second-largest estuarine system on the Kerala coast (located on the SW coast of India), is recognised as a Ramsar site (Ramsar convention of wetlands in 2002) and a potential site for shellfish fishery resources (Babu et al.2010; Chinnadurai et al.2016). Approximately 70 % of bivalve shellfish (molluscs, oysters and clams) harvesting sites on the Kerala coast are reported to be confined to both Ashtamudi and Vembanad estuarine systems (CMFRI, 2016). Nevertheless, recent microbial studies in the AE have documented that this region is being contaminated with faecal indicator bacteria (FIB) and pathogens, mainly associated with wastewater discharges from domestic industrial and agricultural sources (Salahudeen et al.2017; Chinnadurai et al.2020). The drastic escalation of anthropogenic pressures (e.g. land reclamation for urban, industrial and harbour developments) along with ceaseless effluent discharges (both domestic and industrial) have caused the overall water quality deterioration of the AE (Jennerjahn et al.2008; Babu et al.2010). Since shellfishes are exclusively dependent on suspended organic particles in the water column, predominantly on phytoplankton, the changes in phytoplankton community composition can profoundly influence the growth and distribution of these filter-feeding benthic organisms.

Concerning the AE, no coherent information on phytoplankton community dynamics is available, except for random reports based on conventional microscopy measurements (Mathew and Nair, 1980; Nair et al.1984; Jennerjahn et al.2008). These reports are, of course, insufficient to understand the overall growth, distribution, and succession patterns of the phytoplankton community in the AE in correspondence with the prevailing environmental (climate) changes. The majority of estuaries (the largest Cochin estuary, in particular) along the southwest coast of India usually exhibit the preponderance of diatoms almost throughout the year because of the persistent nutrient (mainly

NO<sub>3</sub>-N and PO<sub>4</sub>-P) availability (Menon et al. 2000; Qasim, 2003; Meenu et al. 2021). However, phytoplankton studies in the AE showed the explicit dominance of cyanobacteria (Mathew and Nair, 1980) and chlorophytes (Jennerjahn et al.2008), irrespective of seasons. These results, however, are interpreted using the microscopy based phytoplankton composition data that do not account any qualitative information on small-sized PFGs (e.g., cyanobacteria, chlorophytes, haptophytes etc). Apart from this, the hydrographic properties of the AE showed a distinctive spatio-temporal variation similar to other estuaries in the southwest coast of India mainly because of southwest-induced torrential rainfall and river runoff (Qasim, 2003) and also increasing anthropogenic activities (Jennerjahn et al.2008). These environmental changes also affect the overall phytoplankton community composition and primary productivity. Based on these facts, the present study attempted for the first time to elucidate the spatio-temporal variation of PFGs in the AE and adjacent nearshore waters using HPLC derived biomarkers. In addition, CHEMTAX calculations were implemented to estimate the contribution of major PFGs to the chlorophyll *a* biomass and, subsequently, evaluated the pattern of diversity and succession of major PFGs within various salinity regimes (euhaline, mesohaline and oligohaline) of the study region.

## **2.0 Materials and Methods**

### *2.1 Study area*

The AE is located between 8°52'- 9°28'N and 76°32'-76°41'E, covering an area of 54 km<sup>2</sup> with a total length of 16 km (Babu et al.2010). Because of the shallow depth (< 5 m) condition, this microtidal semidiurnal estuary experiences a tidal range of ~1m. The AE is topographically characterized by a palm-shaped extensive water body with eight prominent pockets/depressions and hence the name 'Ashtamudi' ('Ashta' means eight and 'mudi' means head) (Nair et al.2010; Varghese, 2015). The estuary is open to the Arabian Sea through a permanent narrow inlet (~200 m width) at Neendakara. Major freshwater input to the estuary is from the Kallada River, formed by three small tributaries (i.e. Kulathupuzha, Chendurni and Kalthuruthy), which originated in the uplands of the Western Ghats (Jennerjahn et al.2008). During SWM (June - September), all tributaries of the Kallada River transport an enormous quantity of freshwater into the AE, which is subsequently flushed out to the AS through the Neendakara inlet. By contrast, during the non-monsoon period, the intrusion of neritic waters took place via the Neendakara inlet and transformed the whole estuary into a mesohaline zone (Babu et al.2010). The AE is recognized as one of the major inland water bodies of Kerala, which supports a large-scale shellfish fishery (including populations of oysters, clams and mussels) and commercially harvested to supply national and international markets (CMFRI, 2016; Chinnadurai et al.2021). Recent studies in the AE revealed that

this system has been experiencing severe environmental issues, including pollution from various sources, especially during the non-monsoon seasonal periods when the estuary prevails poor flushing due to the minimum discharge from the Kallada river and its tributaries (Jennerjahn et al.2008; Babu et al.2010; Chinnadurai et al.2020).

## 2.2. Field sampling strategy

Field observations and samplings were carried out in the inner estuary and adjacent nearshore waters (< 20 m depth) during 2018-2019 period in four different seasons, i.e., spring intermonsoon-SIM (April), summer monsoon-SM (July), fall intermonsoon-FIM (November) and winter monsoon-WM (February). The sampling stations were fixed in such a manner that two stations (1-2) in the nearshore waters (15m and 10 m depth, respectively) and 5 stations (3-7) in the estuarine region, extending from the inlet (station 3) to the river mouth (station 7), based on salinity gradients (Fig. 1).

## 2.3. Environmental data and sample analysis

The data (daily average) for the major meteorological parameters (wind speed, atmospheric temperature and rainfall) were retrieved from the site, <https://www.ecmwf.int> and similarly, the river discharge data of the AE was taken from the site <https://indiawris.gov.in>. The vertical profiles of water temperature, salinity, turbidity and photosynthetically active Radiation (PAR) were recorded using a Conductivity-Temperature-Depth profiler (CTD- SBE, Seabird Electronics, USA). Water samples for chemical and biological (phytoplankton pigments) parameters were collected from the near-surface (0.5 m) and near-bottom depths using a Niskin Sampler (5 L capacity). Collected samples were subsequently transferred into clean polyethylene bottles and stored in cool dark iceboxes until reach the laboratory. The major inorganic nutrients, i.e. ammonium (NH<sub>4</sub>-N), nitrite (NO<sub>2</sub>-N), nitrate (NO<sub>3</sub>-N), phosphate (PO<sub>4</sub>-P) and silicate (SiO<sub>3</sub>-Si) were estimated using an autoanalyzer (Skalar san++), following Grasshoff et al. (1983). Subsequent to the nutrient analysis, the water samples (subsamples from the clean polyethylene bottles) were filtered through membrane filters (dia 47 mm; nominal pore size 0.45 µm) under low vacuum (pressure <500 mb) to eliminate detrital particles. The dissolved inorganic nitrogen (DIN) was calculated as the sum of NH<sub>4</sub>-N, NO<sub>2</sub>-N and NO<sub>3</sub>-N. The dissolved oxygen (DO) content in the water samples was estimated following Winkler's titration method using a Metrohm 865 Dosimat Plus.

The phytoplankton chlorophyll *a* concentrations and photo- (marker) pigments were estimated using HPLC analytical method (Van Heukelem, 2002). One to two litres of the water sample, collected from the near-surface and bottom waters, were filtered onto Whatman GF/F filters (nominal pore size 0.7µm; 25mm diameter) under low vacuum (<500 mb), and the filters were then

kept in a deep freezer (-20°C) until the analysis. Before the commencement of analysis, the frozen filters were disrupted for 30 seconds in 4 ml of 90% acetone using a sonicator (Model 100, Fischer Scientific) and the content was later filtered through a syringe filter (25mm dia, nominal pore size 0.2 µm) for removing unwanted debris. The pigment extracts (~ 400 µL) were injected into the HPLC system (Agilent 1100) using a reverse-phase C8 column (150 x 4.6 mm, 3.5µm particle size) with a three-phase solvent gradient at a flow rate of 1.1µL/minutes (van Heukelem, 2002). The absorption spectra of the pigments were measured at two wavelengths, i.e., 450 and 665 nm, using a Diode Array Detector (DAD). The pigments were identified from the absorption spectra and subsequently quantified based on their retention time against standard pigments obtained from DHI® Institute for Water and Environment, Denmark. The abbreviations of phytoplankton marker pigments and various pigment indices used for the present study are depicted in Table 1 (Gibb et al.2001).

#### 2.4. CHEMTAX analysis

The contribution of each phytoplankton functional group (PFG) to the total biomass (chlorophyll *a*; hereafter chl *a*) was estimated using the HPLC-derived pigments by the factorial program of CHEMTAX calculations (Mackey et al.1996; Wright et al.2010). For this purpose, only the surface pigment data have been used as the phytoplankton community along different depths may vary in their pigment to chl *a* ratios (Gibb et al.2001; Mackey et al.1996). The initial pigment ratios for the major PFGs were taken from the literature (Table 2) (Gibb et al.2001; Parab et al.2013; Roy et al.2015). Based on the marker pigments detected from the study, five PFGs (i.e., diatoms, cyanobacteria, chlorophytes, cryptophytes, and dinoflagellates) were loaded to CHEMTAX for SIM and WM seasonal periods. On the other hand, four PFGs (i.e., diatoms, cyanobacteria, chlorophytes, cryptophytes) were considered for SM and FIM periods. Apart from chl *a*, marker pigments such as fucoxanthin, zeaxanthin, lutein, chlorophyll *b*, peridinin and alloxanthin were taken for input values for CHEMTAX calculations during SIM and WM periods; however, for SM and FIM periods, peridinin was excluded from the rest of the pigments mentioned above (Table 3). The diagnostic pigments (DP), which were either absent or observed in trace amounts and also the pigments which have a complex taxonomic distribution (chlorophyll *c*2 and chlorophyll *c*3) were excluded from the CHEMTAX analysis.

#### 2.5 Statistical analysis

The Karl Pearson correlation analyses were performed to find out the linear relationship of salinity and nutrients to the chl *a* and various marker pigments (Table 5; Figure 9). Similarly, student's *t*-test (two-tailed) was done to find out the statistical difference in the means of major

environmental variables and phytoplankton pigments between the seasons (Table 6). In addition, redundancy analysis (RDA) was carried out using the statistical program CANOCO 4.5, to understand the interrelationships between the abiotic and biotic variables. The abiotic variables included were temperature, salinity, turbidity, PAR, pH, DO, and inorganic nutrients ( $\text{NH}_4\text{-N}$   $\text{NO}_3\text{-N}$ ,  $\text{PO}_4\text{-P}$  and  $\text{SiO}_3\text{-Si}$ ) and the biotic variables were chl *a*, marker pigments and PFGs (derived from CHEMTAX calculations). Prior to the analysis, de-trended correspondence analysis (DCA) was carried out to select the most suitable ordination techniques for the present data set. The DCA result showed that the axis gradient length was less than 2 and therefore, the linear multivariate method of RDA was considered the most appropriate for the present data. Biological variables were log-transformed prior to the analysis, and the results of the RDA analysis were presented as a triplot (Fig. 10).

### 3. Results

#### 3.1. Environmental variables

Generally, the atmosphere over the study region was noticeably warmer during the non-monsoon months ( $>28.5\text{ }^\circ\text{C}$ ) compared to the monsoon months ( $<27\text{ }^\circ\text{C}$ ) (Fig. 2a). The wind speed was strikingly higher ( $>7\text{ m s}^{-1}$ ) during the SM and SIM periods and slightly lower ( $<5.7\text{ m s}^{-1}$ ) during the FIM and WM periods (Fig. 2b). Maximum rainfall was recorded during the SM (av.  $16.6 \pm 34.0\text{ mm/day}$ ), followed by FIM ( $7.6 \pm 18.0\text{ mm/day}$ ), whereas the SIM and WM periods were characterized by the occurrence of minimum rainfall (Fig. 2c). Maximum river discharge in the AE was recorded during the SM period (av.  $153 - 307\text{ m}^3/\text{s}$ ), and the minimum was during the SIM period ( $<12\text{ m}^3/\text{s}$ ).

The water column of the whole study region showed a distinctive spatio-temporal variation in the major physico-chemical variables. The water column appeared to be warm ( $>30\text{ }^\circ\text{C}$ ) and well-mixed, especially in the estuary, during the non-monsoon months (except the SM) (3a - 3d). A characteristic horizontal gradient (low to high) in water column temperature was discernible from the near shore to estuarine upper reaches, regardless of seasons. During the SM, comparatively cooler ( $24.5 - 27\text{ }^\circ\text{C}$ ) and well-stratified water column was obvious, particularly in the near shore region (Fig. 3b). Concerning water column salinity, a more or less similar distribution pattern was evident in the whole study region during both SIM and WM periods with the prevalence of higher salinity (34). By contrast, a sharp salinity drop, especially between stations 3 (34) and 7 (5), was evident during the SM. The nearshore waters (stations 1 and 2), on the other hand, constantly sustained high salinity ( $>34$ ), regardless of seasons (Fig. 3e-3h). The water column turbidity was quite distinctive during the

SM period with enhanced levels, especially in the mixing zones, from stations 3 to 5 (>15 NTU) (Fig. 3i-3l). However, the whole study region remained less turbid (<7 NTU) during the non-monsoon periods, and it was more pronounced in the nearshore waters. The availability of water column PAR was relatively higher ( $\sim 100\text{-}2000 \mu\text{E m}^{-2} \text{s}^{-1}$ ) during the non-monsoon periods, especially in the nearshore waters during FM and WM periods, compared to the estuary (Fig. 3).

During most sampling seasons, a well-oxygenated ( $>4 \text{ mg L}^{-1}$ ) water column was observed in the whole study region. However, a pronounced hypoxic ( $<1.5 \text{ mg L}^{-1}$ ) condition, especially at the nearshore stations (1 and 2), was observed during the SM (Figs. 4a). As far as the nutrients are concerned, a marked increase (av.  $18.6 \pm 4.2 \mu\text{M}$ ) in dissolved inorganic nitrogen (DIN) was recorded in the whole study region, especially during the SM period. The  $\text{NH}_4\text{-N}$ , the chief component of DIN, constituted the major N fraction (64-81%) in the estuary, irrespective of seasons, and it was more distinct during the WM period, both in the surface and bottom waters (Figs. 4b). However,  $\text{NO}_3\text{-N}$  formed the major fraction ( $>80\%$ ) of DIN during the SM period in all the sampling stations (Figs. 4c). Generally, the AE was characterized by low levels of  $\text{PO}_4\text{-P}$  ( $<0.5 \mu\text{M}$ ) with minimum spatio-temporal variability (Fig. 4d). The nearshore waters and adjacent estuarine stations sustained slightly higher  $\text{PO}_4\text{-P}$  ( $>1.5 \mu\text{M}$ ), especially during the SM (Fig. 4d). The dissolved  $\text{SiO}_2\text{-Si}$  was consistently higher ( $>30 \mu\text{M}$ ) in the estuary compared to the nearshore waters; nevertheless, a remarkable increase in  $\text{SiO}_2\text{-Si}$  ( $>40 \mu\text{M}$ ) was detected at stations 5 to 7, located near the river mouth, regardless of seasons (Fig. 5e). The nutrient stoichiometry (N:P, Si:N and Si:P ratios) generally found complement with the prevailing nutrient levels (Fig. 5a-5c). The N:P ratio remained well above the normal Redfield ratio (16:1) during the non-monsoon months, particularly inside the estuary (Fig. 5a). However, the Si:N ratio was apparently higher (av.  $>3$ ) throughout the study region than the normal Redfield ratio and it was prominently discernible in the estuary, except during the WM (av.  $2.1 \pm 1$ ) period (Fig 5b). The Si:P ratio was constantly higher (17 - 334) in the whole study region than the normal Redfield ratio (16:1) because of the over saturation of  $\text{SiO}_3\text{-Si}$  regardless of seasons (Fig.5c). Similar to Si:P, overall Si:N ratio remained consistently higher both in the near shore waters (1-4) and estuary (1-12).

### 3.2. Phytoplankton biomass (chl *a*), biomarkers, pigment indices and functional groups

The AE, in general, sustained noticeably higher phytoplankton chl *a* concentrations (av.  $> 5 \text{ mg m}^{-3}$ ) almost throughout the sampling periods both in the surface and bottom waters (Fig. 6). However, stations close to the inlet (3 and 4) showed a distinguishing temporal variation in chl *a*, probably because of the greater influence of neritic waters with variable tidal influence. The nearshore waters, on the other hand, exhibited consistently low levels of chl *a* ( $<1.5 \text{ mg m}^{-3}$ ),



regardless of seasons (Fig. 6). During the SIM period, an exceptional increase in chl *a* was recorded in the estuary both in the surface (av.  $10.17 \pm 1.84 \text{ mg m}^{-3}$ ) and bottom (av.  $9.93 \pm 2.42 \text{ mg m}^{-3}$ ) waters, specifically at stations 4 to 7, located somewhat interior estuary from the inlet. On a seasonal scale, the whole sampling stations sustained noticeably low levels of chl *a* both in the surface (av.  $4.6 \pm 0.70 \text{ mg m}^{-3}$ ) and bottom (av.  $5.52 \pm 1.68 \text{ mg m}^{-3}$ ) waters. Apart from this, an obvious increase in chl *a* ( $> 5 \text{ mg m}^{-3}$ ) was apparent at stations near the river mouth region (5-7), irrespective of seasons.

The phytoplankton marker pigments, in general, showed a specific spatio-temporal variation, especially in its diversity and corresponding concentrations, in the study region (Fig. 7). A distinguishing domination of zeaxanthin (av.  $1.04 \text{ mg m}^{-3}$ ) was evident in the estuary over other marker pigments during the non-monsoon seasonal periods (i.e. SIM, FIM and WM), which was followed by chlorophyll *b* (av.  $0.47 \text{ mg m}^{-3}$ ). However, a nominal increase in fucoxanthin was detected at the estuarine stations (3 and 4), located near the inlet region, especially during the WM (av.  $0.4 \text{ mg m}^{-3}$ ) and SM (av.  $0.2 \text{ mg m}^{-3}$ ) periods (Figs. 7b and 7d). Likewise, a moderate increase in alloxanthin ( $0.5\text{-}1.6 \text{ mg m}^{-3}$ ) was recorded at certain stations (5-7) in the estuary during the SM, both in the surface and bottom waters (Figs. 7g - 7h). Other marker pigments such as lutein ( $<0.2 \text{ mg m}^{-3}$ ), diadinoxanthin ( $< 0.4 \text{ mg m}^{-3}$ ), chlorophyll *c2* ( $<0.5 \text{ mg m}^{-3}$ ), carotenoids ( $<0.1 \text{ mg m}^{-3}$ ), peridinin ( $<0.1 \text{ mg m}^{-3}$ ), chlorophyll *c3* ( $<0.05 \text{ mg m}^{-3}$ ), 19'-hexanoyloxyfucoxanthin ( $<0.02 \text{ mg m}^{-3}$ ), diatoxanthin ( $< 0.07 \text{ mg m}^{-3}$ ), etc. were also detected nominally in the study region, regardless of seasons. The nearshore waters, on the other hand, sustained low levels of marker pigments compared to the estuary (Figs. 7). The quality and quantity of these marker pigments were quite dissimilar in the near shore waters on a temporal scale compared to the estuary and fucoxanthin was the predominant biomarker at this region, regardless of seasons (Fig. 7). Among the photopigment indices, the concentrations of photoprotective carotenoids (PPCs) were apparently higher in the AE compared to the photosynthetic carotenoids (PSCs), almost throughout the sampling seasons (Table 4). The estuary remained a distinguishing dominance of PPCs during the SIM period, both on the surface (av.  $3.29 \pm 0.58 \text{ mg m}^{-3}$ ) and bottom waters (av.  $2.97 \pm 0.94 \text{ mg m}^{-3}$ ). The nearshore waters, however, persisted a marked dominance of PSCs over PPCs, irrespective of seasons (Table 4). The PPC:PSC ratio was distinctly higher in the estuary throughout the sampling period, and prominently higher during the SIM period, especially in the surface waters (Table 4). The seasonal mean of photosynthetic pigments (PSP) and diagnostic pigments (DP) were also conspicuously higher in the estuary, irrespective of seasons, compared to the nearshore waters (Table 4).

The phytoplankton functional group (PFG) dynamics, elucidated based on chl *a* concentrations derived from the CHEMTAX analysis, have revealed the occurrence of six major

PFGs (i.e., cyanophyta, dinophyta, cryptophyta, chlorophyta, bacillariophyta and haptophyta) in the whole study region (Fig. 8). The chl *a* contributions from each PFG showed a clear-cut spatio-temporal variation, wherein a cyanobacterial contribution of chl *a* (~50-80 % of total chl *a*) was highly prominent in the estuary, regardless of seasons, specifically for non-monsoon periods (Figs. 8a,c and d). Besides this, diatoms and chlorophytes appeared to contribute moderate amounts of chl *a* in the estuary. On the other hand, this scenario was quite different during the SM period, wherein the whole sampling stations in the estuary apparently showed the involvement of multiple PFGs towards the contribution of chl *a* (Fig. 8d). Cryptophytes, cyanophytes, bacillariophytes and chlorophytes were those multiple PFGs formed the major chl *a* contributors in the estuary during this season. Moreover, the estuarine stations (specifically 5-7), located in the vicinity of the river mouth region, showed slightly higher chl *a* contributions (~30-50%) found to be derived from mainly cryptophytes (Fig. 8d). The nearshore waters (stations 1 and 2), on the other hand, evident for the significant contribution of chl *a* exclusively from diatoms (45-60%), regardless of seasons, which appeared to be low concentrations as compared to the estuary. Dinoflagellate derived chl *a* was discernible at stations 2 to 6 during the WM period and at the nearshore stations (1 and 2) during the SIM period (Figs. 8a and 8d).

### 3.3. Interrelationships between environmental variables and PFGs

Linear regression analysis, adopted for examining the correlation of salinity and inorganic nutrients (NH<sub>4</sub>-N, NO<sub>3</sub>-N, PO<sub>4</sub>-P and SiO<sub>3</sub>-Si) with phytoplankton photopigments and major PFGs showed variable relationship patterns (Table 5). Salinity (n = 56) in the whole study region showed a significant positive linear correlation with chl *a* ( $p < 0.01$ ), alloxanthin ( $p < 0.01$ ) and chl *c2* ( $p < 0.05$ ), irrespective of seasons. Inorganic nutrients also established significant positive correlations with chl *a*, certain marker pigments and PFGs (Table 5). Likewise, the regression plots between the nutrient ratios (N:P, Si:N and Si:P) and chl *a* clearly demonstrated the non-existence of significant linear correlation ( $p > 0.05$ ) both in the estuary as well as in the nearshore waters (Fig.9). Student's *t*-test (two-tailed) was performed to find out the significance of statistical variation (seasonal scale) between the seasonal means of environmental variables and phytoplankton pigments (Table 6). The seasonal mean of major environmental parameters (e.g., temperature, turbidity, pH, nutrients and nutrient ratios) exhibited significant statistical variation ( $p < 0.05$ ) between each season (Table 6). Similarly, phytoplankton chl *a* and certain marker pigments (e.g., zeaxanthin, peridinine, carotenoids, lutein and chl *b*) were also found to be significantly variable seasonally (Table 6).

The RDA plot has shown unique interrelationship patterns between the environmental variables and major biomarkers and their corresponding PFGs (Fig.10). Cyanobacteria, cryptophytes

and chlorophytes exhibited a significant positive correlation with  $\text{SiO}_3\text{-Si}$ , temperature and nutrient ratios (i.e. N:P, Si:N and Si:P), especially at the estuarine stations (mainly 5-7) during SIM, SM and FM periods. During the WM period, on the other hand, multiple environmental variables such as PAR, pH,  $\text{NH}_4\text{-N}$ , temperature and  $\text{SiO}_3\text{-Si}$  showed a significant positive correlation with dinoflagellates and certain marker pigments (peridinin, diadinoxanthin and diatoxanthin), mainly at stations 4-7, located away from the inlet. The diatoms and haptophytes, and also the corresponding biomarkers, showed a positive correlation with a suite of environmental variables (i.e.  $\text{NO}_3\text{-N}$ ,  $\text{PO}_4\text{-P}$ ,  $\text{NO}_2\text{-N}$ , DO, salinity and turbidity) and this particular scenario was evident at stations 1 and 2 in the nearshore waters, irrespective of seasons (Fig. 10).

#### 4. Discussion

The AE, one of the potential sites for the commercially important shellfishes (mussels, oysters, clams) on the southwest coast of India, is reported to contribute ~ 70% of the total shellfish resources in Kerala state, along with the Vembanad lake system (CMFRI, 2016). Nevertheless, as per recent reports, the AE has been on the verge of faster water quality deterioration, including overgrowth of pathogenic bacterial populations, as a result of the intensifying anthropogenic pressures, mainly because of the incessant discharge of wastewater from domestic industrial sources and also runoff from agricultural areas (Babu et al.2010; Salahudeen et al.2018; Chinnadurai et al. 2020).The present study, mainly concerning phytoplankton marker pigment dynamics of the AE and adjacent nearshore waters, has unfolded various anomalies of phytoplankton communities in association with the seasonally driven environmental hydrographic changes, mainly by the tide-induced seawater incursion and river influx. Besides, the study has elucidated the spatial variability of pigment compositions and associated PFGs in the various salinity regimes (i.e. euhaline, mesohaline and oligohaline) of the study region.

Normally, the southwest coast of India experiences maximum solar irradiance and concomitant high evaporation rates during the non-monsoon seasonal periods, SIM (March-mid May), in particular (Qasim, 2003). Consequently, the nearshore waters of the SW coast of India, including estuaries, experience characteristic warm and high salinity conditions. The present study also evidenced such environmental scenarios in the AE with the presence of warm ( $>29.5^\circ\text{C}$ ) and high salinity (20-35) waters, especially during the non-monsoon seasonal periods. The gradients in salinity (high to low) noticeable in the study region (nearshore to the estuary) during these seasons indicate the prevalence of large-scale incursion of neritic waters into the estuary (Fig.3). This condition was more prevalent during the SIM and WIM periods as the obvious salinity rise (28) in the upper regions (station 7) of the estuary apparently pointed towards the occurrence of minimum

river discharge. By contrast, hydrological features of the AE were quite dissimilar during the SM period, especially at stations 5 to 7, located in the vicinity of river mouth (Fig.3f). The drastic drop in salinity ( $<10$ ) was found to be mainly driven by the prevailing torrential monsoonal rainfall and concomitant terrestrial runoff as reported earlier in the estuaries along the SW coast of India (Menon et al., 2000; Qasim, 2003; Madhu et al.2007). In fact, this salinity drop in the upper reaches of the AE was primarily facilitated by the huge influx from the Kallada River and its tributaries. In nearshore waters, on the other hand, a sharp temperature drop ( $25^{\circ}\text{C}$ ) was clearly discernible during this season compared to the estuary (Fig. 3b). This temperature drop in the surface layers of stations 1 and 2 was found to be associated with the influence of seasonally occurring coastal upwelling phenomena as reported earlier (Madhupratap et al.1990; Muraleedharan et al., 2018). The presence of cool ( $<25^{\circ}\text{C}$ ), less oxygenated ( $<2\text{ mg L}^{-1}$ ) and nutrient-rich ( $\text{NO}_3\text{-N}>7.5\text{ }\mu\text{M}$  and  $\text{PO}_4\text{-P}>1\text{ }\mu\text{M}$ ) waters detected in the nearshore stations categorically uphold the influence of coastal upwelling phenomenon, a recognized recurrent coastal oceanographic phenomenon, in the southwest coast of India during the SM period. In addition to this, the conspicuous turbidity maxima ( $>20\text{ NTU}$ ) confined at the estuarine stations (mainly between 3 and 4), specifically during this season, indicated the influence of the profound mixing of two hydrographically different waters (neritic waters and freshwaters) (Fig. 3j).

As in any other estuaries along the southwest coast of India, inorganic nutrient levels in the AE were also recorded to be consistently higher (Qasim 2003; Madhu et al.2007, Martin et al.2008). Nevertheless, the present study has shown a distinguishable spatio-temporal variation in the distribution of inorganic nutrients as well as its stoichiometric ratios in the AE (Figs. 4 and 5). Previous observations also documented the prevalence of large-scale spatio-temporal variations in inorganic nutrients in the AE, as a result of the intense influence of environmental changes in the prevailing hydrology, geology and land use (Jennerhahn et al. 2008, Babu et al., 2010). Concerning the DIN levels, the AE sustained a major fraction of  $\text{NH}_4\text{-N}$  ( $\sim >70\%$ ) all over during the non-monsoon periods (WM in particular) and it was reported due to the supersaturation of  $\text{NH}_4\text{-N}$  because of the persistent inputs from either anthropogenic sources (sewage wastewater and agricultural runoff) or sediment ammonification process (Jennerjahn et al.2008; Salahudeen et al.2018). As per the report, the sediments in shallow estuaries habitually synthesize  $\text{NH}_4\text{-N}$  ions from negatively charged particles by the saltwater effect and also ion-pairing effect (Seitzinger et al.1991). The governance of high salinity waters in the AE during the non-monsoon seasonal periods explicitly reveals the prevalence of poor flushing from the Kallada River. Perhaps, this particular hydrographic scenario might have amplified the process of ammonification in the surficial sediments of the estuary

and subsequent rise of  $\text{NH}_4\text{-N}$  levels in the water column (Fig. 3). A recent study by Salahudeen et al (2018) documented the enhancement of water column  $\text{NH}_4\text{-N}$  in the AE as a result of prevailing ammonification process in surficial sediments and this condition was prevalent in the estuary during the non-monsoon period, when the system sustained high salinity waters. In the present study, this  $\text{NH}_4\text{-N}$  enriched condition in the water column of the whole study region (both AE and nearshore waters) was so evident during the WM period. Similarly, the conspicuous decrease in  $\text{NH}_4\text{-N}$  ( $<3 \mu\text{M}$ ) detected in the estuary, particularly at stations near the river mouth (5-7) during the SM period, can be linked to the prevailing salinity drop due to the enhanced river discharge. In fact, the process of ion-pairing and seawater cation effects could be the fundamental cause of the incessant  $\text{NH}_4\text{-N}$  release from the surficial sediments in estuaries and coastal waters, especially when these systems experience high salinity fluctuations (Seitzinger et al.1991).

The pronounced spatio-temporal variations evidenced in the physico-chemical properties of the whole study region apparently reflected in its phytoplankton characteristics as well. In fact, even though both sampling regimes (estuary and nearshore waters) remain greatly varied in phytoplankton properties spatio-temporally, such variability was highly discernible only in the estuary because of its extreme hydrographic inconsistencies (Fig. 3). The remarkable increase in chl *a* (av.  $> 5 \text{ mg m}^{-3}$ ) observed in the AE, compared to the nearshore waters (av.  $<1.5 \text{ mgm}^{-3}$ ), has pointed out towards the prevalence of conducive environmental conditions (mainly high nutrient levels) for enhanced phytoplankton growth. However, during the SM, the influence of seasonally driven turbidity maximum ( $>20 \text{ NTU}$ ), evident particularly at station 4, appeared to cause a drastic decrease in phytoplankton chl *a* ( $<2 \text{ mg m}^{-3}$ ). The observed plumes of subsurface turbidity maximum at these stations (3 to 6) obviously signify the prevalence of strong vertical mixing of both seawater and river water (Fig. 3j). However, the enhanced chl *a* concentrations recorded at these stations (except station 4) revealed that the prevailing turbidity maximum was not sufficient enough to limit attenuation of PAR as well as phytoplankton growth in the water column even during the SM period (Figs. 3n and 6). Although the hydrochemical properties, mainly the distribution of inorganic nutrient compositions, showed a distinct spatio-temporal variation in the AE, that variability was not translated into making the distinguishable changes in phytoplankton chlorophyll *a* biomass in the estuary, especially during the non-monsoon seasons compared to the nearshore waters (Fig.6). However, unlike other major estuaries along the west coast of India wherein diatoms usually dominates (Roy et al.2006; Meenu et al. 2021), the AE sustained a widespread increase in zeaxanthin which apparently signifies the preponderance of cyanobacterial populations during most of the sampling periods. According to previous studies, cyanobacteria usually exhibit wide compositional

variability in coastal waters worldwide, including the estuaries and adjacent inland waters, because of the prevailing hydrological discrepancies (Mur et al.1999; Paerl et al.2020). The Cochin estuary, for example, exhibits the numerical dominance of diatoms almost throughout the year due to the surplus availability of inorganic nutrients, especially  $\text{NO}_3\text{-N}$  and  $\text{PO}_4\text{-P}$  (Menon et al. 2000; Madhu et al. 2007). Recent HPLC-based biomarker studies categorically evidenced the super-saturation of fucoxanthin in the Cochin estuary, irrespective of seasons, which apparently substantiated the preponderance of diatoms (Meenu et al, 2021). However, the nutrient status of the present study has shown that  $\text{NH}_4\text{-N}$  was the predominant inorganic N component in the AE, particularly during the non-monsoon seasons, along with the occurrence of apparent P limitation as evidenced from the N:P and Si:P ratios (Fig.4 and 5). Therefore, the constant increase in  $\text{NH}_4\text{-N}$  can be considered one of the major triggering factors of the consistently enhanced growth of cyanobacterial populations in the AE during the non-monsoon periods. In marine ecosystems, cyanobacteria populations constitute the most dominant prokaryotic fraction of the phytoplankton community, specifically belonging to two major genera *Prochlorococcus* or *Synechococcus* (Partensky et al.1999). Usually, these prokaryotic autotrophic communities prefer to grow in warm coastal marine waters, especially when nutrient-depleted (mainly  $\text{NO}_3\text{-N}$  and  $\text{PO}_4\text{-P}$ ) condition prevails (Wang et al.2011; El-Shehawy et al.2012). The present study, however, has documented the preponderance of the cyanobacterial community in the AE based on the recorded concentrations of its biomarker, zeaxanthin. Nevertheless, since the AE apparently lacks information on cyanobacterial predominance (especially flowcytometry data), it was rather difficult to characterize the prevailing cyanobacterial taxa (genus or species). Recent reports on flow cytometry-derived picophytoplankton composition data generated from the estuaries of the southwest coast of India have documented a distinctive numerical abundance of *synechococcus* compared to other cyanobacterial communities (Mohan et al.,2016; Rajaneesh et al.,2020). Concerning *synechococcus* community, two major strains have been identified yet based on the type of pigment in cells, for example, phycocyanin (PC) rich *synechococcus* (PC-SYN) and phycoerythrin (PE) rich *synechococcus* (PE-SYN) (Paerl et al. 2020). The PC-SYN often numerically dominate in relatively low salinity waters (<25), whereas the PE-SYN tend to proliferate in high salinity (>25) waters (Wang et al.2011). On the basis of these facts, it can be inferred that the remarkable increase in zeaxanthin in the AE, almost throughout the sampling periods, may have originated from *synechococcus*, as tropical estuaries are reported to sustain a high abundance of this cyanobacterial taxa, especially during the warm periods (El-Shehawy et al.2012; Mohan et al.2016; Rajaneesh et al.,2020). Furthermore, the pervasiveness of high salinity conditions in the AE along with the dominance of zeaxanthin over other marker pigments, especially during the non-monsoon months, categorically unveils that the cyanobacterial populations in the estuary might be PE-SYN

rich strains as this particular *synechococcus* strain prefer to grow in high salinity waters (Wang et al.2011; Mohan et al.2016). The occurrence of high salinity waters in the AE, along with high chl *a* contribution derived from the cyanobacterial community, infers that PE-SYN could be the major *synechococcus* strain in the AE, especially during non-monsoon seasons.

In any aquatic system, an estuary in particular, the inorganic nutrient levels and corresponding stoichiometric element ratios play a vital role in determining the growth and diversity of phytoplankton communities (Justic et al.1995; Gardner et al.2009). The formation of harmful algal blooms (HABs) and the concurrent eutrophication processes in estuaries are normally regarded as manifestations of nutrient enrichment (Cloern et al.2014). Most estuaries on the southwest coastline of India exhibit a distinct seasonality in the nutrient stoichiometry, and phytoplankton growth in these estuaries are identified to be mostly N-limited, mainly NO<sub>3</sub>-N (Table.7). The prevailing seasonality in the river discharge has a profound influence on nutrient distributions in these estuaries, especially during the monsoon season when all the rivers in southwestern India carry enormous quantities of freshwater together with huge amounts of suspended sediments and both organic and inorganic materials (Qasim 2003; Madhu et al.2007; Jennerjahn et al. 2008). As far as the AE is concerned, the present study has shown the establishment of high N:P and Si:P ratios, especially during the warm seasonal periods. These anomalies in the nutrient ratios ultimately signified P limitation for phytoplankton growth, particularly for diatoms (Fig. 6a and 6c). Normally, nutrient preferences of phytoplankton are reported to be group specific; diatoms usually prefer growing in NO<sub>3</sub>-N rich waters, whereas chlorophytes and cyanobacteria tend to grow in NH<sub>4</sub>-rich environments (Justic et al.1995; Gardner et al.2006). The preference for NH<sub>4</sub>-N by cyanobacteria is fundamentally associated with the low energy requirement for their assimilation compared to the NO<sub>3</sub>-N. The conspicuous increase of NH<sub>4</sub>-N detected in the AE, exclusively during the non-monsoon periods, can be considered as one of the potential causes of the overall preponderance of cyanobacterial populations in the estuary. At the same time, although the exact source of NH<sub>4</sub>-N in the AE is unknown, based on the previous reports, it can be assumed that high ammonification rates in the sediments (Giblin et al.2010) as well as the tremendous increase in sewage wastewater and agricultural runoff (Salahudeen et al.2018), could be the possible sources of NH<sub>4</sub>-N in the AE. The hydrographic profiles, especially the salinity, observed during the non-monsoon seasonal periods, clearly indicated the pervasiveness of high salinity (> 25) waters all along the study region, and ultimately, this high salinity waters may have accelerated the ammonification rates in the sediments as reported earlier (Salahudeen et al., 2018).

In the nearshore waters, the vertical profiles of hydro-chemical properties appeared to be quite similar almost throughout all the sampling periods, except during the SM, wherein a slight difference in hydro-chemical properties was discernible because of the influence of coastal upwelling process (Fig.3b and 3f). This marginal seasonal variation of hydro-chemical properties observed in the nearshore waters was reflected in the phytoplankton chl *a* concentrations as well. The occurrence of consistently low levels of chl *a* ( $< 1.5 \text{ mg m}^{-3}$ ) in this region, regardless of seasons, pointed towards the diminished growth of phytoplankton. Simultaneously, the quality and quantity of marker pigment concentrations were relatively low in the nearshore waters compared to the AE, irrespective of seasons. However, unlike the AE, the nearshore waters sustained a distinctive dominance of fucoxanthin ( $>0.1 \text{ mg m}^{-3}$ ) over other marker pigments throughout the sampling periods, which apparently signified the numerical dominance of diatoms. The results of CHEMTAX data also substantiated the dominance of fucoxanthin in contributing chl *a* to ( $>80\%$ ) the total chl *a* pool (Fig. 8). Indeed, the preponderance of diatoms all along the nearshore waters ( $<30 \text{ m}$ ) of the southwest coast of India, almost throughout the year, was a piece of established information (Patil and Anil, 2015; Minu et al.2014; Madhu et al.2021). Concerning the pigment indices, the obvious dominance of higher PPCs over PSCs all over the AE, signifies the prevalence of environmental stress conditions during the non-monsoon seasonal periods, which are apparently not conducive to the growth of diatoms (Barlow et al. 2007). The consistent availability of enhanced nutrient levels, particularly  $\text{NO}_3\text{-N}$  and  $\text{PO}_4\text{-P}$  (major precursors of diatom growth), were the crucial precursors for the persistent dominance of diatoms in the nearshore waters of southwestern India (Qasim et al., 2003; Madhu et al., 2017). Recent studies on phytoplankton marker pigments by HPLC technique have already substantiated the preponderance of diatoms in these regions by detecting high concentrations of fucoxanthin (Roy et al.2006; Parab et al.2013; Madhu et al.2020). Nevertheless, apart from diatoms, the occurrence of sporadic blooms of certain dinoflagellates (e.g. *Noctiluca scintillans*, *Prorocentrum shikokuense*, *Karenia mikimotoi*) and prymensiophytes (e.g. *Phaeocystis globosa*) indicated the influence of climate-induced environmental changes on potential PFGs (Sahayak et al.2005; Padmakumar et al.2010; Madhu et al., 2020).

Even though the AE exhibited a noticeable dominance of zeaxanthin over other biomarkers, especially during the non-monsoon months, this scenario was not discernible during the SM period. Instead, the estuarine stations, specifically stations 5 to 7, showed the dominance of alloxanthin along with moderate amounts of fucoxanthin, zeaxanthin and chl *b* (Fig.7). The CHEMTAX results subsequently revealed the co-occurrence of multiple PFGs (e.g., cryptophytes, diatoms, cyanobacteria and chlorophytes, respectively) in these stations, corresponding to their biomarkers in



terms of chl *a* contributions (Fig. 8). The substantial increase in river influx evident in the AE by the presence of low salinity waters (<7), in connection with the torrential monsoonal rainfall and runoff, have caused the decline in cyanobacterial populations during this season. The obvious sharp salinity drop evident in the estuary (especially at stations 5 to 7), along with noticeable rise in NO<sub>3</sub>-N and PO<sub>4</sub>-P may have led to the growth of multiple PFGs of freshwater preference in the AE during the SM period. All the above-mentioned PFGs usually prefer to grow in NO<sub>3</sub>-N and PO<sub>4</sub>-P rich waters rather than NH<sub>4</sub>-N. On the other hand, the clear-cut dominance of cyanobacteria in the AE (mainly the upper reaches), which occurred during the non-monsoon seasonal periods, was found to be associated with the enhanced tide induced seawater incursion, as shown in the salinity profiles (Fig. 3). The seasonal trends in inorganic nutrients, especially the consistent increase in NH<sub>4</sub>-N could be identified as one of the significant triggering factors for the cyanobacterial growth in the AE. As mentioned in the previous sections, diatoms constituted the predominant PFG in most of the estuaries on the southwest coast of India (for example, Cochin estuary and Zuari-Mandovi estuaries) almost throughout the year as a result of the constant availability of inorganic nutrients, mainly NO<sub>3</sub>-N and PO<sub>4</sub>-P (Madhu et al., 2010; Patil et al., 2015; Meenu et al., 2021). However, in the AE, the present study has evidenced the substantial decrease in PO<sub>4</sub>-P and also NO<sub>3</sub>-N (to some extent), except during the SM period (Fig.4). Moreover, the obvious enhancement of N:P and Si:P ratios in the estuary, especially during the non-monsoon seasonal periods, revealed the prevalence of significant P limitation in the water column (Fig. 5) and perhaps, this P limitation could be one of the major causes of limited growth of diatoms in the AE, especially during the non-monsoon seasonal periods.

In this study, various statistical analyses (linear regression, Student's *t*-test and RDA) have been adopted to delineate the existing interrelationships between the environmental variables and phytoplankton pigment properties (Tables 5 and 6; Figs. 9 and 10). All these statistical analyses, however, were unable to interpret the proper establishment of significant relationships between the environmental variables and phytoplankton properties in the whole study region. Probably, the characteristic geomorphological asymmetry as well as the dynamic hydrographic properties of the AE could be the possible reasons for the lack of significant correlations between the physico-chemical parameters and phytoplankton properties. However, the results of the RDA analysis have shown a significant positive correlation of cyanobacteria (also chlorophytes and cryptophytes) with temperature, silicate and nutrient ratios, especially at stations located in the proximity of the river mouth during the non-monsoon seasonal periods (Fig 10). Even the results of linear correlation analysis between the nutrient ratios and chl *a* concentrations, did not show any significant correlation ( $p>0.05$ ) patterns in the study region (Fig. 9). However, the results of Student's *t*-test revealed the

prevalence of significant seasonal variation of certain environmental parameters (e.g., temperature, turbidity, pH, nutrients and nutrient ratios) with phytoplankton marker pigments (Table 6). Since the AE is known as one of the major potential shellfish fishery resources in the Kerala state (CMFRI, 2016; Chinnadurai et al.2021), the information on phytoplankton community dynamics, especially on its functional composition and succession patterns with respect to the prevailing environmental changes, even if based on HPLC derived marker pigments, will be highly beneficial to understand the current status of the estuary in terms of phytoplankton productivity. Concerning AE, such measurements on phytoplankton community dynamics are first of its kind and hence, the information brought out from this study has its own significance, especially for understanding the prevailing biogeochemical processes and the estuarine pollution.

## **5. Conclusion**

The present study on phytoplankton marker pigments has evidenced a characteristic preponderance of cyanobacterial communities in the AE, particularly during the non-monsoon seasonal periods, based on the chl *a* contribution from each PFG estimated by the CHEMTAX analysis. The pervasiveness of warm (>29 °C) waters (as a result of shallow depth), along with enhanced inorganic NH<sub>4</sub>-N, may have prompted the preponderance cyanobacterial community in the AE, especially during the SIM, FIM and WM seasonal periods when high salinity (>25) conditions prevailed. The obvious P limitation in the AE, evidenced by the nutrient ratios (N:P and Si:P), appeared to have a significant role in the limited growth of conventional larger phytoplankton taxa, for example, diatoms and dinoflagellates in the estuary. However, the consistent dominance of fucoxanthin observed in the nearshore waters (although lower concentrations compared to the estuary), regardless of seasons, indicated the preponderance of diatoms, wherein NO<sub>3</sub>-N was recorded to be the leading inorganic nutrient. On the basis of the present study, it can be categorically stated that HPLC-CHEMTAX data was highly useful for understanding phytoplankton community dynamics in the study region. Also, it could provide information not only on the chl *a* contribution of each PFG but also on the small-sized or fragile groups of taxonomic importance more precisely than any other analysis available. Since the AE was designated as a Ramsar site and an ideal ground for economically important shellfish resources, periodical monitoring of water quality, even by implementing HPLC-based pigment studies, should be promoted to resolve the possible local environmental management problems that affect the natural growth of phytoplankton communities.

## Acknowledgements

The authors thank Director, NIO, Goa and Scientist-in-Charge, NIO-Regional Centre Kochi, for their constant encouragement and support. The authors also thankful to Dr. Muraleedharan K. R and Mr. Abdul Azeez S, who have assisted by providing meteorological data for the present study. The corresponding author acknowledges the Science and Engineering Research Board (SERB), Government of India, New Delhi for providing financial support for carrying out this work.

## Declaration

**Ethics approval:** The manuscript does not contain any studies with human participants or animals performed by any of the authors.

**Consent to participate:** Not applicable

**Consent for publication:** Not applicable

Availability of data and materials: Not applicable

**Competing interests:** The authors declare that there is no competing interest.

**Funding:** The study was supported by the SERB New Delhi as part of the project EMEQ.

Author's contribution: **P. Anil** - Sample analysis, data processing, original draft writing, **N. V. Madhu** - Conceptualization, Methodology, writing and editing of original draft, **C. R. Vishal** - Sample analysis and data processing, **P. Gopika** - Sample analysis data processing, **S. Jyothi** - Sample analysis data processing, **K. S. Arya** - Sample analysis and data processing, **T. R. Gireeshkumar** - Data processing & editing.

## References

Agusti S, Lubián LM, Moreno-Ostos E, Estrada M, Duarte CM (2019) Projected changes in photosynthetic picoplankton in a warmer subtropical ocean. *Front Mar Sci* 5, 506.

Ankit Y, Mishra PK, Kumar P, Jha DK, Kumar VV, Ambili V, Anoop A (2017) Molecular distribution and carbon isotope of n-alkanes from Ashtamudi Estuary, South India: Assessment of organic matter sources and paleoclimatic implications. *Mar Chem* 196, 62-70.

Anooja S, Padmalal D, Maya K, Mohan SV, Baburaj B (2013) Heavy mineral contents and provenance of Late Quaternary sediments of southern Kerala, Southwest India. *Indian J Mar Sci* 42(6), 749-757.

Babu KN, Omana PK, Mohan M (2010) Water and sediment quality of Ashtamudi estuary, a Ramsar site, southwest coast of India-a statistical appraisal. *Environmental Monitoring and Assessment* 165, 307–319. <https://doi.org/10.1007/s10661-009-0947-0>.

- Banse K (1959) On upwelling and bottom-trawling off the southwest coast of India. *J Mar Biol Assoc India* 1, 33-49.
- Barlow R, Kyewalyanga M, Sessions H, van den Berg M, Morris T (2008) Phytoplankton pigments, functional types, and absorption properties in the Delagoa and Natal Bights of the Agulhas ecosystem. *Estuar Coast Shelf Sci* 80, 201–211.
- Bharathi MD, Sarma VV (2019) Impact of monsoon-induced discharge on phytoplankton community structure in the tropical Indian estuaries. *Reg Stud Mar Sci* 31:100795.
- Bhavya PS, Kumar S, Gupta GV, Sudheesh V (2017) Carbon uptake rates in the Cochin estuary and adjoining coastal Arabian Sea. *Estuaries Coast* 40(2):447-56.
- Bijoy Nandan S, Jayachandran PR, Sreedevi OK (2014) Spatio-temporal pattern of primary production in a tropical coastal Wetland (Kodungallur-Azhikode Estuary), South West Coast of India. *J Coast Dev* 17:392.
- Birks HJB (1998) DG Frey and ES Deevey Review 1: Numerical tools in palaeolimnology—Progress, potentialities, and problems. *J Paleolimnol* 20(4), 307-332.
- Cavalcanti LF, Cutrim MV, Lourenço CB, Sá AK, Oliveira AL, de Azevedo-Cutrim AC (2020) Patterns of phytoplankton structure in response to environmental gradients in a macrotidal estuary of the Equatorial Margin (Atlantic coast, Brazil). *Estuarine, Coastal and Shelf Science*. 245:106969.
- Chinnadurai S, Campos CJA, Geethalakshmi V, Sharma J, Kripa V, Mohamed KS (2020) Microbiological quality of shellfish harvesting areas in the Ashtamudi and Vembanad estuaries (India): Environmental influences and compliance with international standards. *Mar Pollut Bull* 156, 111255. <https://doi.org/10.1016/j.marpolbul.2020.111255>.
- Chinnadurai S, Campos CJA, Geethalakshmi V, Kripa V, Mohamed KS (2021) Baseline health risk assessment of trace metals in bivalve shellfish from commercial growing areas in the estuaries of Ashtamudi and Vembanad (Kerala, India). *Environ Sci Pollut Res* 28(48), 68338-68348.
- Chowdhury M, Hardikar R, Kesavan HC, Thomas J, Mitra A, Rokade MA, Naidu VS, Sukumaran S (2017) Nutrient stoichiometry and freshwater flow in shaping of phytoplankton population in a tropical monsoonal estuary (Kundalika Estuary). *Estuar Coast Shelf Sci* 198:73-91.
- Cloern JE, Foster SQ, Kleckner AE (2014) Phytoplankton primary production in the world's estuarine-coastal ecosystems. *Biogeosciences* 7;11(9):2477-2501.
- CMFRI (2016) Central Marine Fisheries Research Institute-Annual Report. Kochi, Kerala, India.
- Elser JJ, Goldman CR (1991) Zooplankton effects on phytoplankton in lakes of contrasting trophic status. *Limnol Oceanogr* 36(1), 64-90.
- El-Shehawy R, Gorokhova E, Fernandez-Pinas F, del Campo FF (2012) Global warming and hepatotoxin production by cyanobacteria: What can we learn from experiments? *Water Res* 46(5), 1420-1429.
- Flombaum P, Gallegos JL, Gordillo RA, Rincón J, Zabala LL, Jiao N, Karl DM, Li WK, Lomas MW, Veneziano D Vera CS (2013) Present and future global distributions of the marine Cyanobacteria *Prochlorococcus* and *Synechococcus*. *Proc Natl Acad Sci U.S.A.* 110(24), 9824-9829.

- Gardner WS, Seitzinger SP, Malczyk JM (1991) The effects of sea salts on the forms of nitrogen released from estuarine and freshwater sediments: does ion pairing affect ammonium flux? *Estuaries* 14(2), 157-166.
- Garmendia M, Borja Á, Franco J, Revilla M (2013) Phytoplankton composition indicators for the assessment of eutrophication in marine waters: present state and challenges within the European directives. *Mar Pollut Bull* 66(1-2), 7-16.
- Gaulke AK, Wetz MS, Paerl HW (2010) Picophytoplankton: A major contributor to planktonic biomass and primary production in a eutrophic, river-dominated estuary. *Estuar Coast Shelf Sci* 90, 45–54.
- Gibb SW, Cummings DG, Irigoien X, Barlow RG, Fauzi R, Mantoura C (2001) Phytoplankton pigment chemotaxonomy of the northeastern Atlantic. *Deep Sea Res Part II Top Stud Oceanogr* 48, 795–823.
- Giblin AE, Weston NB, Banta GT, Tucker J, Hopkinson CS (2010) The effects of salinity on nitrogen losses from an oligohaline estuarine sediment. *Estuaries Coasts* 33(5), 1054-1068.
- Gireeshkumar TR, Mathew D, Pratihary AK, Naik H, Narvekar KU, Araujo J, Balachandran KK, Muraleedharan KR, Thorat B, Nair M, Naqvi SWA (2017) Influence of upwelling induced near shore hypoxia on the Alappuzha mud banks, South West Coast of India. *Cont Shelf Res* 139, 1-8.
- Grasshoff K, Ehrhardt MKK (1983) *Methods of Seawater Analysis*. In: Grasshoff K, Ehrhardt M, Kremling K. (eds.), Verlag Chemie, Weinheim 89 - 224.
- Jabir T, Vipindas PV, Jesmi Y, Valliyodan S, Parambath PM, Singh A, Abdulla MH (2020) Nutrient stoichiometry (N: P) controls nitrogen fixation and distribution of diazotrophs in a tropical eutrophic estuary. *Mar Pollut Bull* 151:110799.
- James MR, Forsyth DJ (1990) Zooplankton-phytoplankton interactions in a eutrophic lake. *J Plankton Res* 12(3), 455-472.
- Jeffrey SW, Mantoura R, Wright S (Eds.) (1997) *Phytoplankton Pigments in Oceanography. Guidelines to Modern Methods*. UNESCO.
- Jeffrey SW, Wright SW, Zapata M (1999) Recent advances in HPLC pigment analysis of phytoplankton. *Mar Fresh Res* 50, 879-896.
- Jennerjahn TC, Soman K, Ittekkot V, Nordhaus I, Sooraj S, Priya RS, Lahajnar N (2008) Effect of land use on the biogeochemistry of dissolved nutrients and suspended and sedimentary organic matter in the tropical Kallada River and Ashtamudi estuary, Kerala, India. *Biogeochemistry* 90, 29–47. <https://doi.org/10.1016/j.ecss.2004.02.008>.
- John S, Revichandran C, Muraleedharan KR, Srijith B, Seena G, Azeez A (2020) Current asymmetry and its implications for morphological changes in Vembanad Lake, the second largest wetland ecosystem in India. *Estuar Coast Shelf Sci* 246, 107013. <https://doi.org/10.1016/j.ecss.2020.107013>.
- Justic D, Rabalais NN, Turner RE, Dortch Q (1995) Changes in nutrient structure of river-dominated coastal waters: stoichiometric nutrient balance and its consequences. *Estuar Coast Shelf Sci* 40, 339–356.

- Lepš J, Šmilauer, P (2003) Multivariate analysis of ecological data using CANOCO. Cambridge university press.
- Mackey MD, Mackey DJ, Higgins HW, Wright SW (1996) CHEMTAX-a program for estimating class abundances from chemical markers: application to HPLC measurements of phytoplankton. *Mar Ecol Prog Ser* 144, 265–283.
- Madhu NV, Jyothibabu R, Balachandran KK, Honey UK, Martin GD (2007) Monsoonal impact on planktonic standing stock and abundance in a tropical estuary (Cochin backwaters India). *Estuar. Coast Shelf Sci* 73(1-2), 54-64.
- Madhu NV, Balachandran KK, Martin GD, Jyothibabu R, Thottathil SD, Nair M, Joseph T, Kusum KK (2010) Short-term variability of water quality and its implications on phytoplankton production in a tropical estuary (Cochin backwaters-India). *Environ Monit Assess* 170(1):287-300.
- Madhu NV, Anil P, Gireeshkumar TR, Muraleedharan KR, Kiran K, Vishal CR (2020) Phytoplankton characterisation in the Alappuzha mud banks during the pre-/post phases of a red-tide, *Prorocentrum shikokuense* Hada. *Regional Studies in Marine Science* 40:101486 <https://doi.org/10.1016/j.rsma.2020.101486>.
- Madhu NV, Anil P, Meenu P, Gireeshkumar TR, Muraleedharan KR, Rehitha TV, Dayana M Vishal CR (2021) Response of coastal phytoplankton to upwelling induced hydrological changes in the Alappuzha mud bank region, southwest coast of India. *Oceanologia* 63(2), 261-275.
- Madhupratap M, Nair SRS, Haridas P, Padmavati G (1990) Response of zooplankton to physical changes in the environment: coastal upwelling along the central west coast of India. *J Coast Res* 413–426.
- Martin GD, Vijay JG, Laluraj CM, Madhu NV, Joseph T, Nair M, Gupta GVM, Balachandran KK (2008) Fresh water influence on nutrient stiochiometry in a tropical estuary, South West coast of India. *Appl ecol environ res* 6(1), 57–64.
- Mathew T, Nair N B (1980). Phytoplankton of the Ashtamudi Estuary, Kerala. *Ind J Mar Sci*, 9, 253-257.
- Meenu P, Madhu NV, Ullas N, Vineetha G, Rehitha TV, Ashwini R, Nair M, Anil P (2021). Characterization of phytoplankton size-structure based productivity, pigment complexes (HPLC/CHEMTAX) and species composition in the Cochin estuary (southwest coast of India): special emphasis on diatoms. *Oceanologia*, 63 (9), DOI: 10.1016/j.oceano.2021.05.004.
- Minu P, Shaju SS, Muhamed Ashraf P, Meenakumari B (2014) Phytoplankton community characteristics in the coastal waters of the southeastern Arabian Sea. *Acta Oceanologica Sinica*, 33(12):170-9.
- Mohamed KS, Sasikumar G (2017) Provisional guidelines for bivalve farming in India with emphasis on meeting hygiene and public health. In: *Aqua Aquaria India*, 113–125.
- Mohan AP, Jyothibabu R, Jagadeesan L, Lallu KR, Karnan C (2016) Summer monsoon onset-induced changes of autotrophic pico-and nanoplankton in the largest monsoonal estuary along the west coast of India. *Environ Monit Assess* 188, 93.

- Mur R, Skulberg OM, Utkilen H (1999) Cyanobacteria in the environment. In: A guide to their public health consequences, monitoring and management. Chorus, I., Bartram, J.E. (Eds.), Spon, London 15-40.
- Muraleedharan KR, Dinesh Kumar PK, Prasanna Kumar S, John S, Srijith B, Anil Kumar K, Naveen Kumar K, Gautham S, Samiksha V (2018) Formation mechanism of mud bank along the Southwest Coast of India. *Estuaries and Coasts* 41(4):1021-35.
- Nair PN, Gopinathan CP, Balachandran VK, Mathew KJ, Regunathan A, Rao DS, Murty A.V.S (1984) Ecology of mudbanks-phytoplankton productivity in Alleppey mudbank. *CMFRI Bulletin* 31, 28-35.
- Nair KM, Padmalal D, Kumaran KP, Sreeja R, Limaye RB, Srinivas R (2010) Late quaternary evolution of Ashtamudi–Sasthamkotta lake systems of Kerala, south west India. *Journal of Asian Earth Sciences* 37(4):361-72.
- Obolewski K, Glińska-Lewczuk K, Kobus S (2009) Effect of hydrological connectivity on the molluscan community structure in oxbow lakes of the Łyna River. *Oceanol Hydrobiol Stud* 38(4), 75-88.
- Padmakumar KB, SreeRenjima G, Fanimol CL, Menon NR, Sanjeevan VN (2010) Preponderance of heterotrophic *Noctiluca scintillans* during a multi-species diatom bloom along the southwest coast of India. *International Journal of Oceans and Oceanography* 4(1):55-63.
- Paerl RW, Venezia RE, Sanchez JJ, Paerl HW (2020) Picophytoplankton dynamics in a large temperate estuary and impacts of extreme storm events. *Scientific reports*. 10(1):1-5.
- Paerl HW, Valdes LM, Pinckney JL, Piehler MF, Dyble J, Moisander PH (2003) Phytoplankton photopigments as indicators of estuarine and coastal eutrophication. *BioScience* 53(10), 953-964.
- Paerl HW, Rossignol KL, Hall SN, Peierls BL, Wetz MS (2010) Phytoplankton community indicators of short-and long-term ecological change in the anthropogenically and climatically impacted Neuse River Estuary, North Carolina, USA. *Estuaries and Coasts*. 33(2):485-97.
- Parab SG, Matondkar SGP, Gomes HR, Goes JI (2013) Effect of Freshwater Influx on Phytoplankton in the Mandovi Estuary (Goa, India) during Monsoon Season: Chemotaxonomy. *J Water Resour Prot* 5, 349–361.
- Partensky F, Blanchot J, Lantoin F, Neveux J, Marie D (1996) Vertical structure of picophytoplankton at different trophic sites of the tropical northeastern Atlantic Ocean. *Deep Sea Res Part I Oceanogr Res Pap* 43(8), 1191-1213.
- Partensky F, Blanchot J, Vaultot D (1999) Differential distribution and ecology of *Prochlorococcus* and *Synechococcus* in oceanic waters: a review. *Bulletin de l'institut océanographique de Monaco*, (spécial 19), pp.457-475.
- Patil JS, Anil AC (2015) Effect of monsoonal perturbations on the occurrence of phytoplankton blooms in a tropical bay. *Mar Ecol Prog Ser* 530, 77–92.
- Qasim SZ (2003) Indian estuaries. Allied publishers. Pvt. Ltd., Heriedia Marg, Ballard Estate, Mumbai.

- Quinlan EL, Philips EJ (2007) Phytoplankton assemblages across the marine to low-salinity transition zone in a blackwater dominated estuary. *Journal of Plankton Research* 29(5):401-16.
- Rajaneesh KM, Naik RK, Roy R, D'Costa PM (2020) Cyanobacteria in tropical and subtropical marine environments: bloom formation and ecological role. In: Singh PK, Kumar A, Singh VK, Shrivastava AK. (Eds.), *Advances in cyanobacterial biology*, 35-46.
- Rath AR, Mitbavkar S, Anil AC (2018) Phytoplankton community structure in relation to environmental factors from the New Mangalore Port waters along the southwest coast of India. *Environ Monit Assess* 190 (8):481. doi: 10.1007/s10661-018-6840-y.
- Raven JA, (1998) The twelfth Tansley Lecture. Small is beautiful: the picophytoplankton. *Funct Ecol* 12(4), 503-513.
- Richardson K (1997) Harmful or exceptional phytoplankton blooms in the marine ecosystem. In *Advances in marine biology Vol 31*, pp 301-385 Academic Press.
- Roy R, Pratihary A, Mangesh G, Naqvi SWA (2006) Spatial variation of phytoplankton pigments along the southwest coast of India. *Estuar Coast Shelf Sci* 69 (1-2), 189-195.
- Roy R, Chitari R, Kulkarni V, Krishna MS, Sarma VVSS, Anil AC (2015) CHEMTAX-derived phytoplankton community structure associated with temperature fronts in the northeastern Arabian Sea. *J Mar Syst* 144, 81-91.
- Sahayak S, Jyothibabu R, Jayalakshmi KJ, Habeebrehman H, Sabu P, Prabhakaran MP, Jasmine P, Shaiju P, Rejomon G, Threslamma J, Nair KK (2005) Red tide of *Noctiluca miliaris* off south of Thiruvananthapuram subsequent to the 'stench event' at the southern Kerala coast. *Current Science* 89, 1472 –1473.
- Salahudeen JH, Reshmi RR, Anoop Krishnan K, Ragi MS, Vincent SGT (2018) Denitrification rates in estuarine sediments of Ashtamudi, Kerala, India. *Environ Monit Assess* 190(6), 1-16.
- Sarma VV, Gupta SN, Babu PV, Acharya T, Harikrishnachari N, Vishnuvardhan K, Rao NS, Reddy NP, Sarma VV, Sadhuram Y, Murty TV (2009) Influence of river discharge on plankton metabolic rates in the tropical monsoon driven Godavari estuary, India. *Estuar Coast Shelf Sci* 85(4):515-24.
- Seitzinger SP, Gardner WS, Spratt AK (1991) The effect of salinity on ammonium sorption in aquatic sediments: implications for benthic nutrient recycling. *Estuaries* 14(2), 167-174.
- Tripathy SC, Ray AK, Patra S, Sarma VV (2005) Water quality assessment of Gautami-Godavari mangrove estuarine ecosystem of Andhra Pradesh, India during September 2001. *J Earth Syst Sci* 114(2):185-90.
- Hans Utermöhl (1958) Methods of collecting plankton for various purposes are discussed., *SIL Communications*, 1953-1996, 9:1, 1-38, DOI: 10.1080/05384680.1958.11904091.
- Van Heukelem L, Thomas CS (2001) Computer-assisted high-performance liquid chromatography method development with applications to the isolation and analysis of phytoplankton pigments. *J Chrom A* 910:31-49.



Van Heukelem L (2002) HPLC phytoplankton pigments: sampling, laboratory methods, and quality assurance procedures. In: Mueller, J., Fargion, G. (Eds.), *Ocean Optics Protocols for Satellite Ocean Colour Sensor, Revision 3: NASA Technical Memorandum 2002-2004* (Chapter 16), 2, 258-268.

Varghese TI (2015). *Sedimentology and geochemistry of core sediments from the Ashtamudi estuary and the adjoining coastal plain, central Kerala, India*. PhD Thesis, Cochin University of Science and Technology, Cochin.

Vijith V, Sundar D, Shetye SR (2009) Time-dependence of salinity in monsoonal estuaries. *Estuar Coast Shelf Sci* 85(4), 601-608.

Wang K, Wommack KE, Chen F (2011) Abundance and distribution of *Synechococcus* spp. and cyanophages in the Chesapeake Bay. *Applied and environmental microbiology* 77(21):7459-68.

Wetz MS, Paerl HW, Taylor JC, Leonard JA (2011) Environmental controls upon picophytoplankton growth and biomass in a eutrophic estuary. *Aquat Microb Ecol* 63(2), 133-143.

Winkler LW (1888) The determination of dissolved oxygen. *Ber Dtsch Chem Ges* 21, 2843-2846.

Wright SW, Jeffrey SW (2006) Pigment markers for phytoplankton production. In *Marine organic matter: biomarkers, isotopes and DNA*. 71-104. Springer, Berlin, Heidelberg.

Wright SW, van den Enden RL, Pearce I, Davidson AT, Scott FJ, Westwood KJ (2010) Phytoplankton community structure and stocks in the Southern Ocean (30-80 E) determined by CHEMTAX analysis of HPLC pigment signatures. *Deep Sea Research Part II: Topical Studies in Oceanography* 57(9-10), pp.758-778.

Figure 1. Details of the study region and sampling locations.

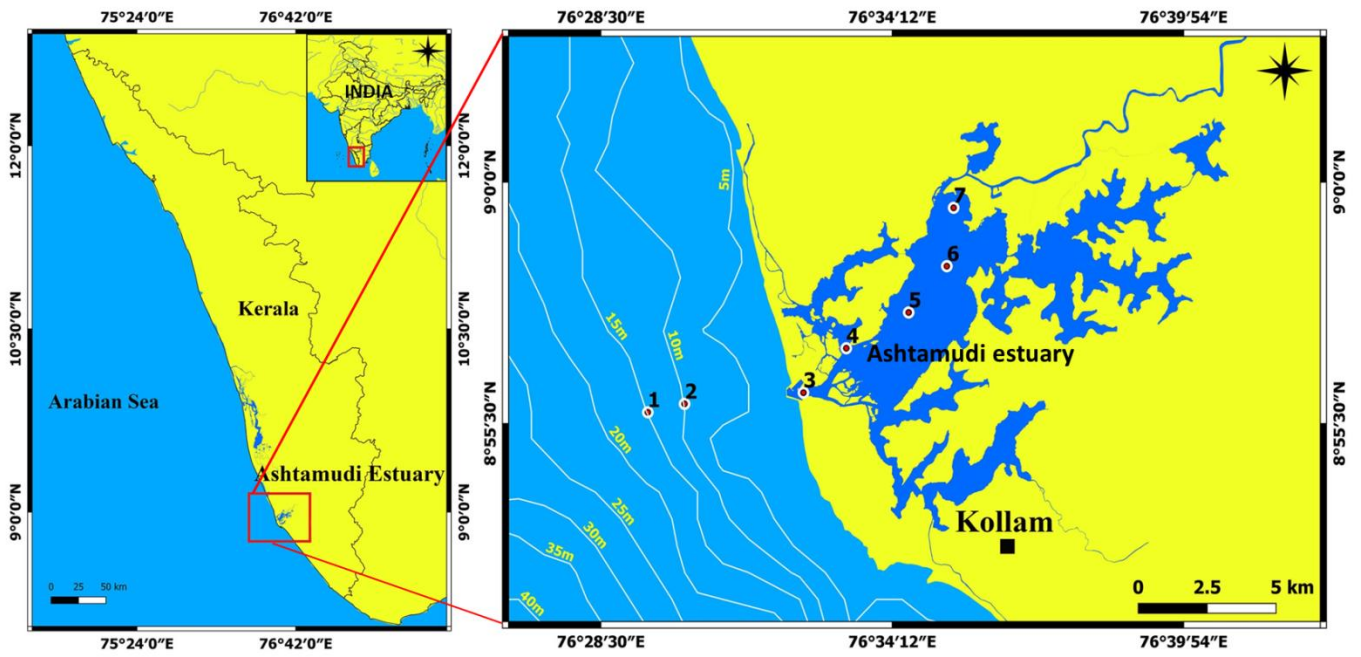


Figure 2. Major climatological parameters (air temperature, wind speed and precipitation) and river discharge during February 2018 to February 2019 from the study region (daily average).

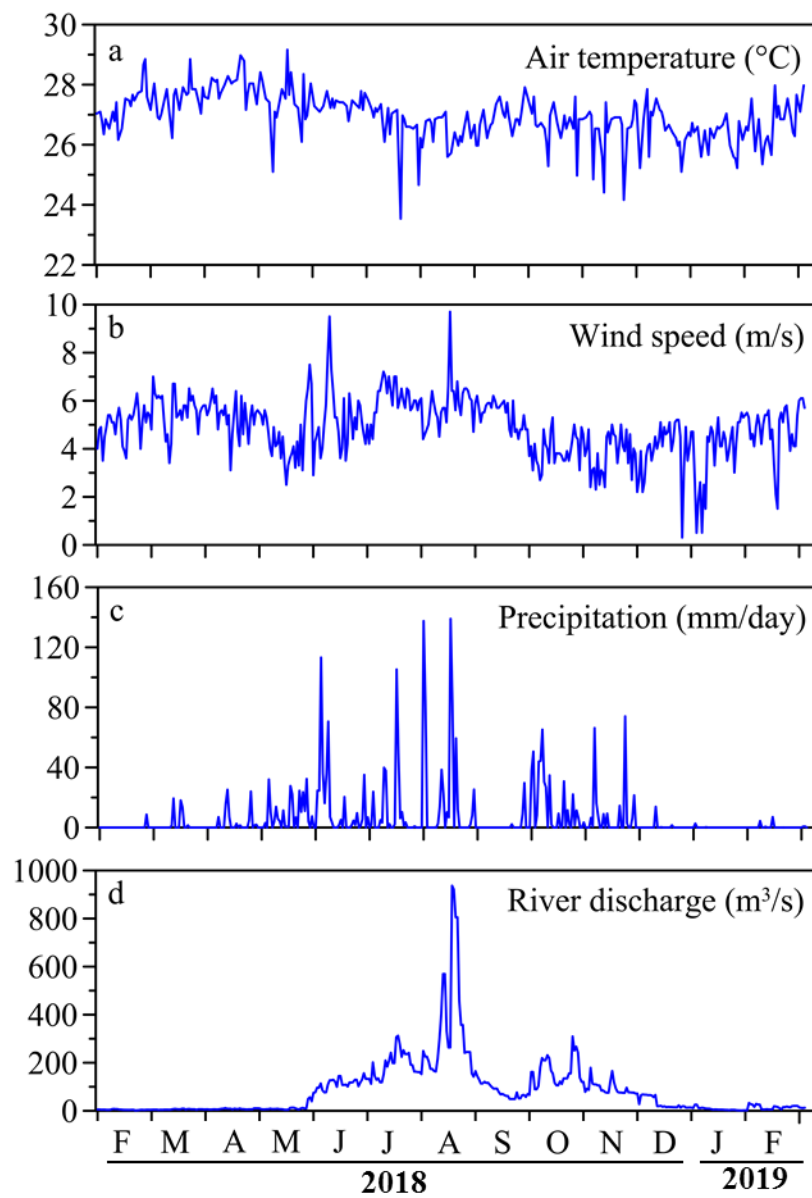


Figure 3. Vertical distribution (seasonal) of temperature (a-d), salinity (e-h), turbidity (i-l) and PAR (m-p) in the Ashtamudi estuary and adjacent coastal waters.

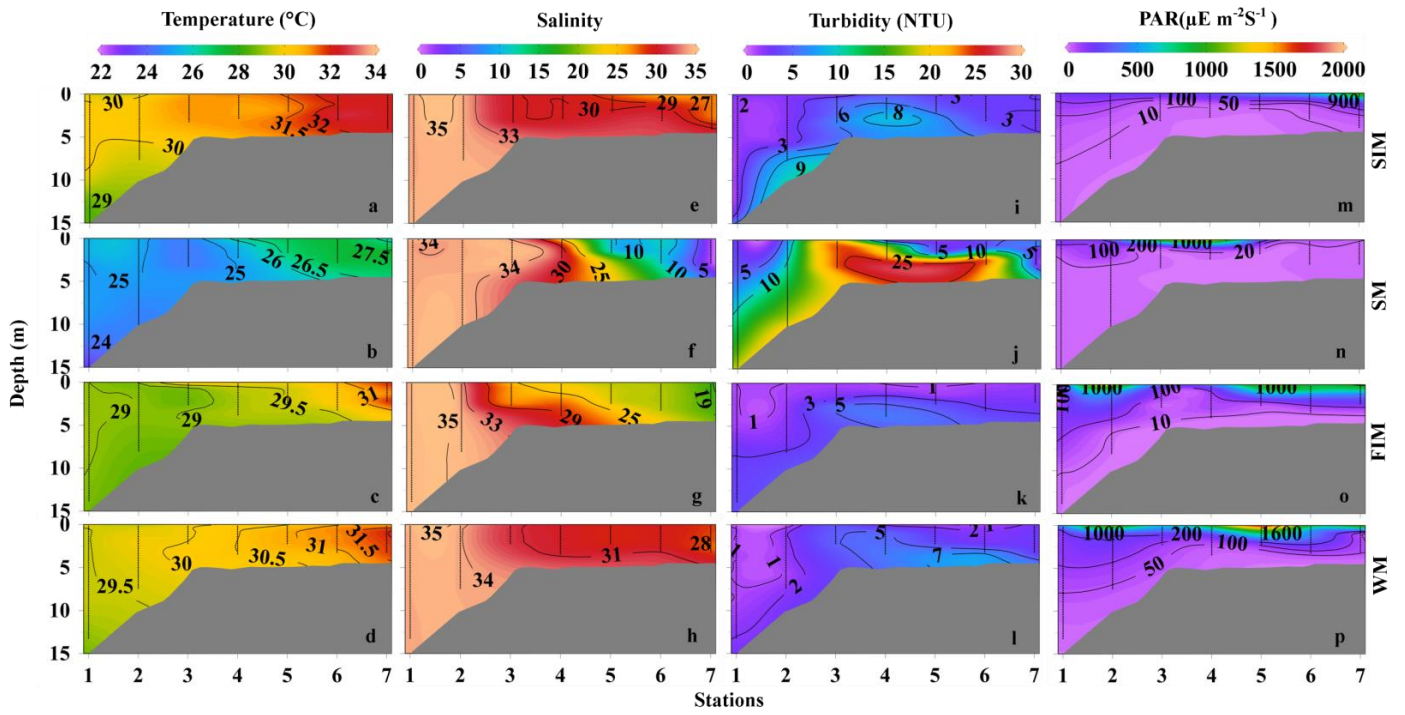


Figure 4. Seasonal distribution of dissolved oxygen and major inorganic nutrients in the Ashtamudi estuary and adjacent coastal waters.

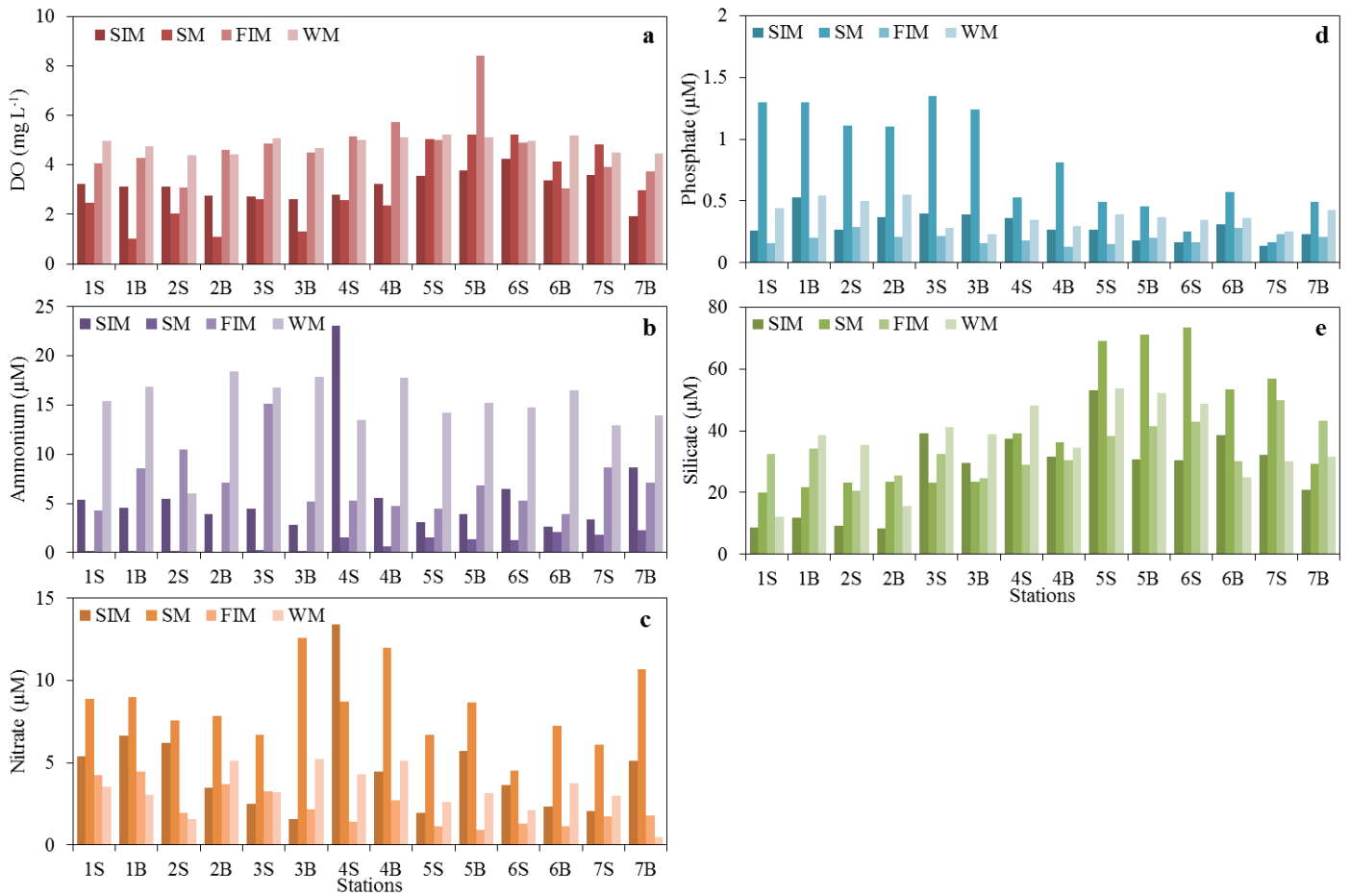


Figure 5. Seasonal nutrient ratios in the surface and bottom waters of Ashtamudi estuary and adjacent coastal waters.

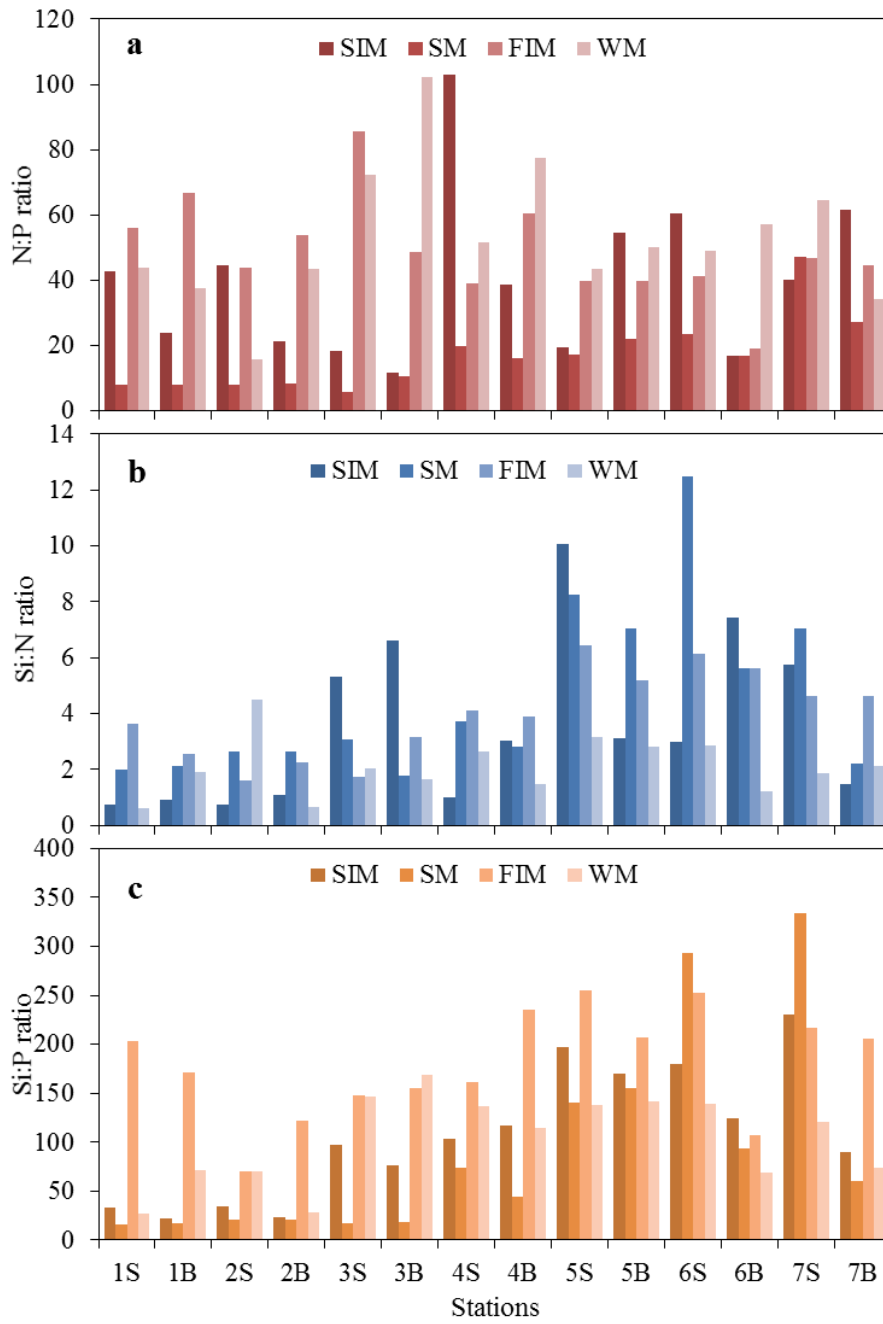


Figure 6. Seasonal distribution of phytoplankton chlorophyll *a* (surface and bottom) in the Ashtamudi estuary and adjacent coastal waters.

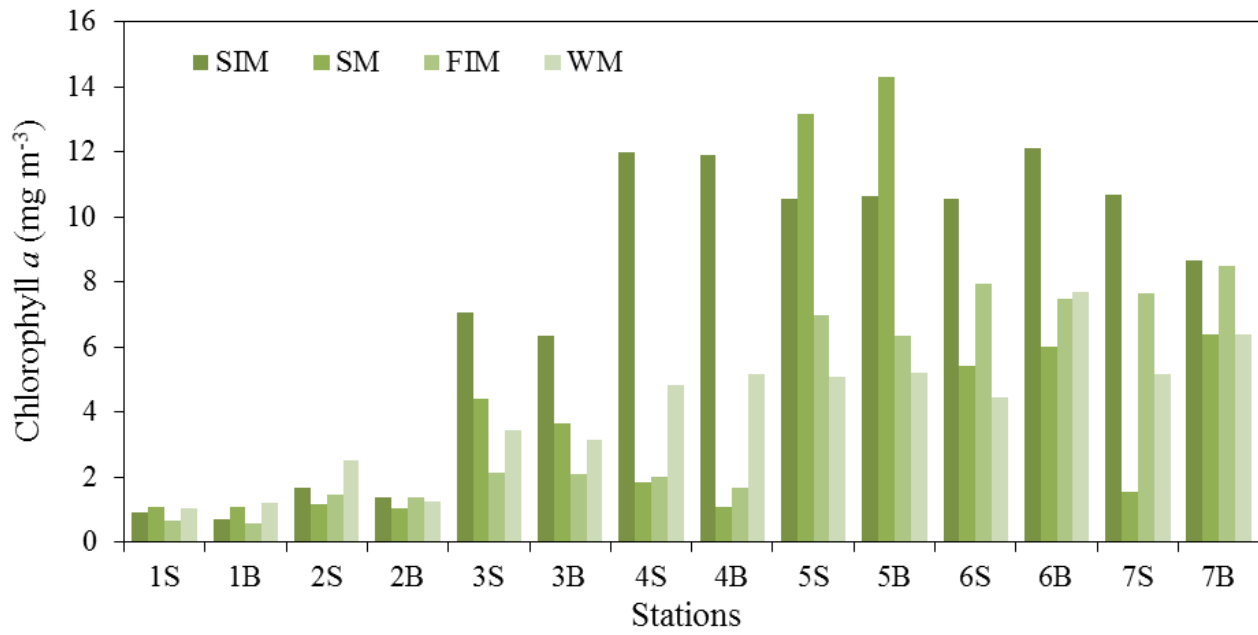


Figure 7. Seasonal distribution of major phytoplankton marker pigments in the Ashtamudi estuary and adjacent coastal waters.

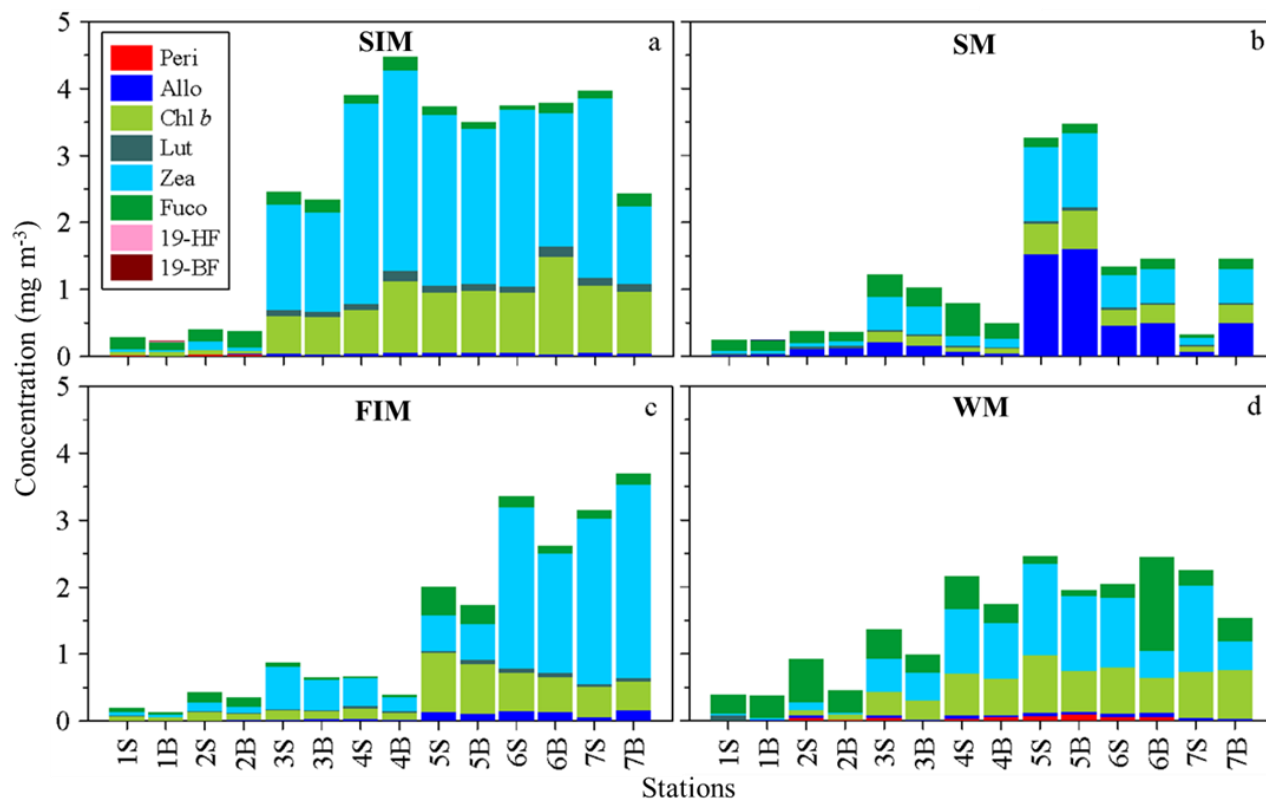




Figure 8. Percentage (%) contribution of chlorophyll *a* (CHEMTAX derived) from major phytoplankton functional groups (PFGs) in the Ashtamudi estuary and adjacent coastal waters.

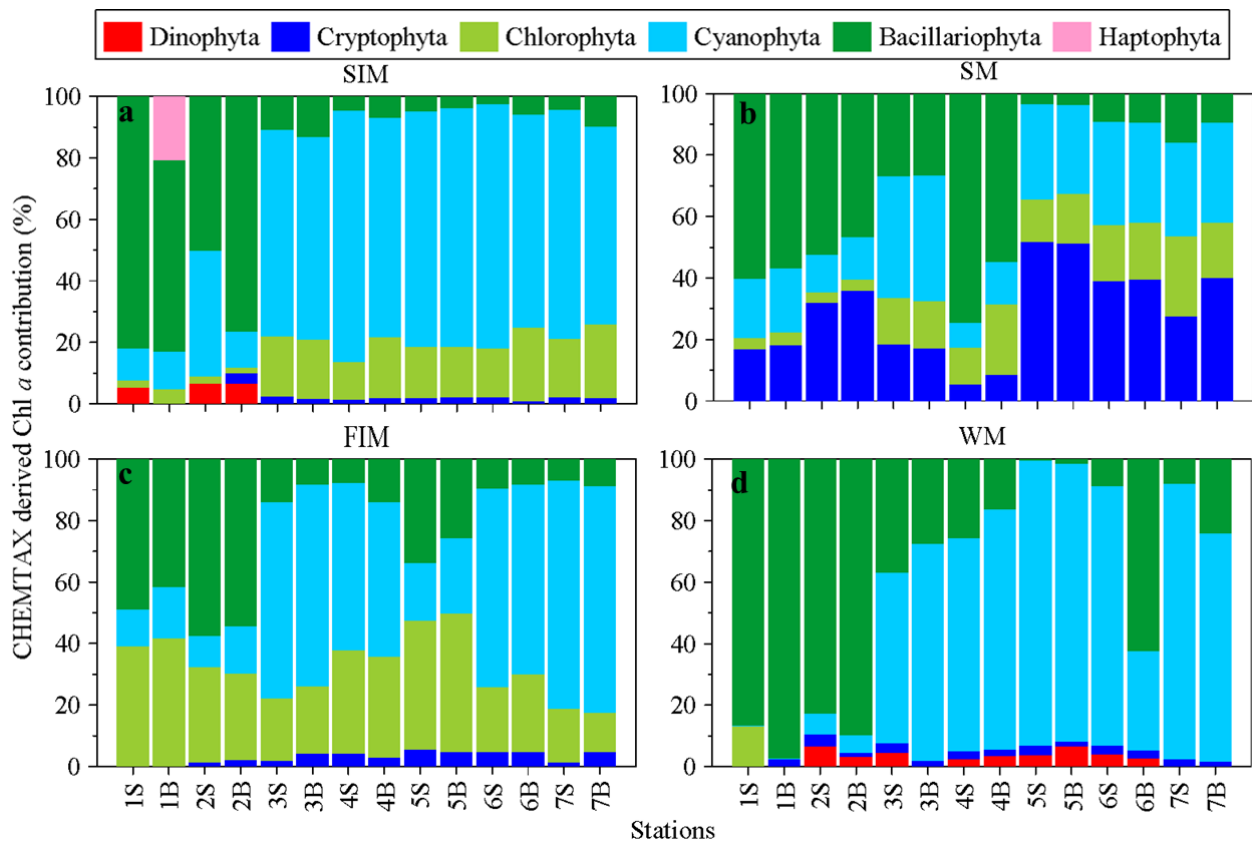


Figure 9. Linear correlation of inorganic nutrient ratios (N:P, Si:N and Si:P) with chlorophyll *a* in the Ashtamudi estuary and adjacent coastal waters.

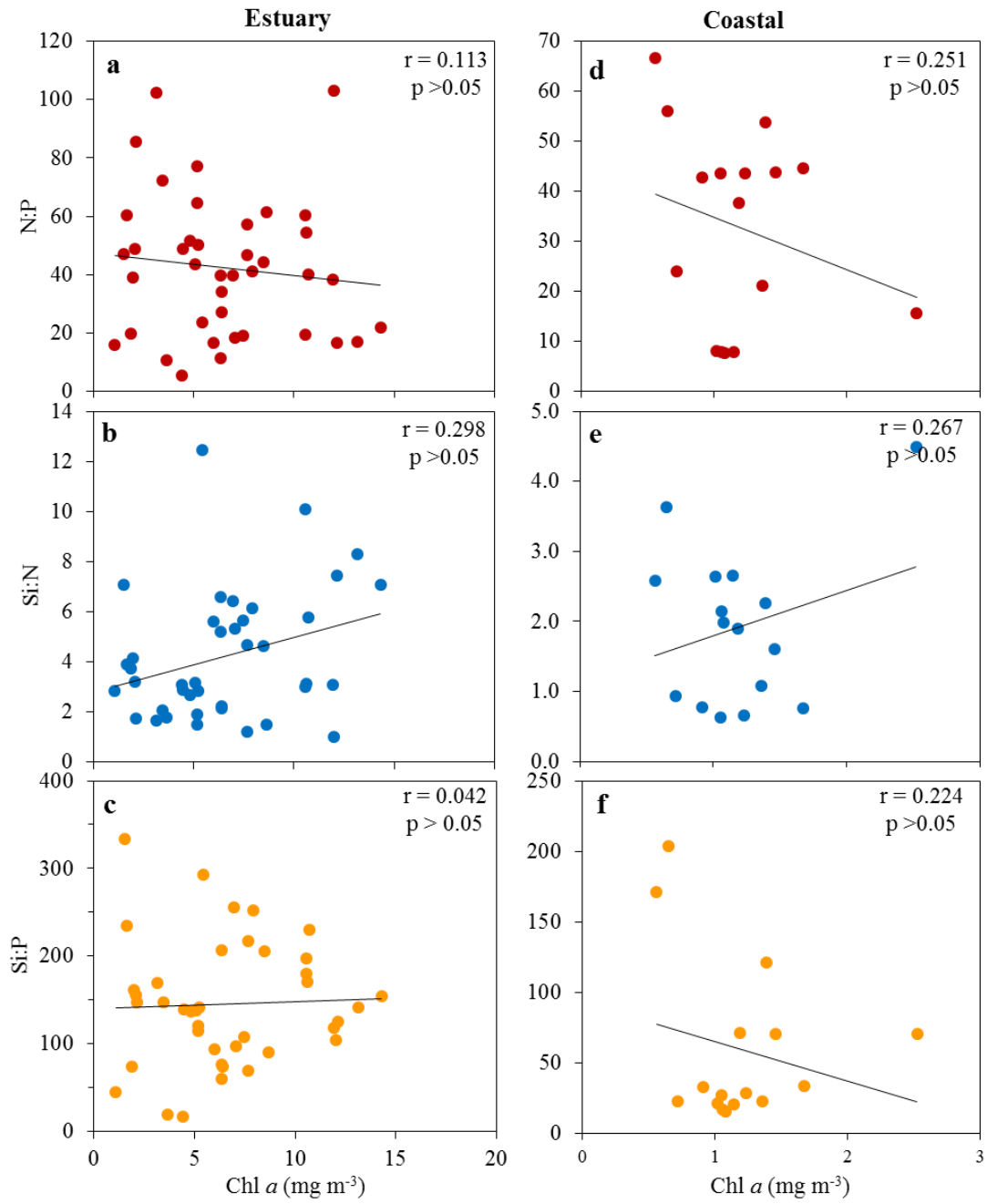


Figure 10. RDA triplot showing the interrelationships between the physico-chemical variables and major biomarkers, and associated phytoplankton functional groups (PFGs) in the Ashtamudi estuary and adjacent coastal waters.

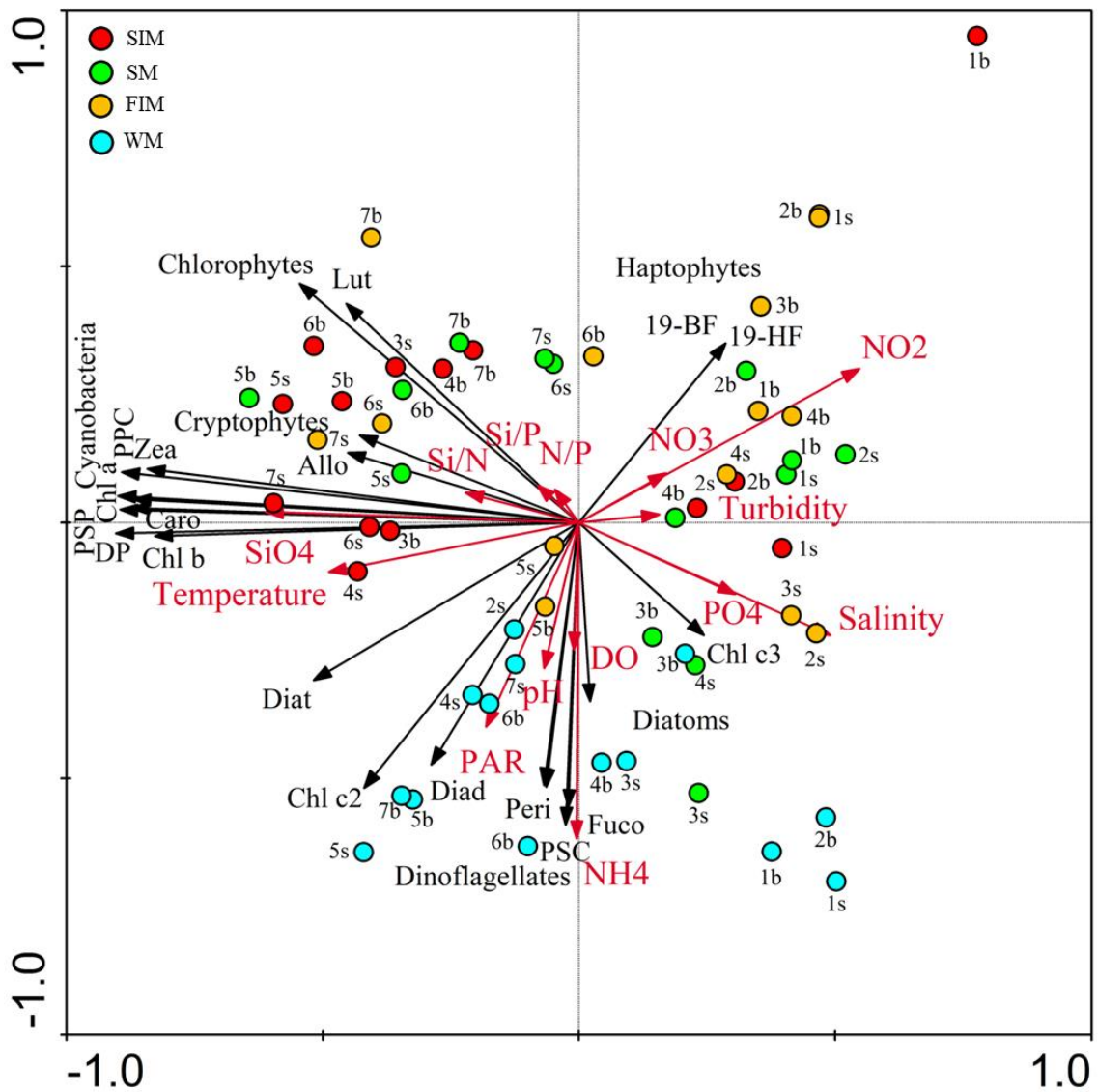


Table 1. Abbreviations, names and formulae for the pigments used for this study (\*Gibb et al.2001)

<b>Abbreviation</b>	<b>Name</b>	<b>Formulae</b>
Allo	Alloxanthin	
Chl <i>a</i>	Chlorophyll <i>a</i>	
Chl <i>b</i>	Chlorophyll <i>b</i>	
Chl <i>c2</i>	Chlorophyll <i>c2</i>	
Chl <i>c3</i>	Chlorophyll <i>c3</i>	
Diad	Diadinoxanthin	
Diat	Diatoxanthin	
Fuco	Fucoxanthin	
19-BF	19'-Butanoyloxyfucoxanthin	
19-HF	19'-Hexanoyloxyfucoxanthin	
Lut	Lutein	
Neo	Neoxanthin	
Per	Peridinin	
Viol	Violaxanthin	
Zea	Zeaxanthin	
Caro	$\beta$ -carotene	
PPC*	Photoprotective Carotenoids	Allo + Diad + Diat + Lut + Neo + Viol + Zea + Caro
PSC*	Photosynthetic carotenoids	Fuco + 19-BF + 19-HF + Peri
DP*	Total Diagnostic Pigments	PSC + Allo + Zea + Chl <i>b</i>

Table 2. Input marker pigments to chlorophyll *a* ratios used for the CHEMTAX calculations (‘-’ Not considered).

<b>Class/Pigment</b>	<b>Peri</b>	<b>Fuco</b>	<b>Allo</b>	<b>Lut</b>	<b>Zea</b>	<b>Chl b</b>	<b>But</b>	<b>Hex</b>	<b>Chl <i>a</i></b>
<b>Initial Ratio Matrix</b>									
<i>Spring Intermonsoon</i>									
Dinoflagellates	0.29	0	0	0	0	0	0	0	1
Cryptophytes	0	0	0.23	0	0	0	0	0	1
Chlorophytes	0	0	0	0.10	0.01	0.15	0	0	1
Cyanobacteria	0	0	0	0	0.19	0	0	0	1
Diatoms	0	0.17	0	0	0	0	0	0	1
Haptophytes	0	0.08	0	0	0	0	0.1	0.15	1
<i>Summer monsoon</i>									
Cryptophytes	-	0	0.19	0	0	0	-	-	1
Chlorophytes	-	0	0	0.10	0.01	0.15	-	-	1
Cyanobacteria	-	0	0	0	0.16	0	-	-	1
Diatoms	-	0.17	0	0	0.00	0	-	-	1
<i>Fall Intermonsoon</i>									
Cryptophytes	-	0	0.20	0	0	0	-	-	1
Chlorophytes	-	0	0	0.10	0.02	0.15	-	-	1
Cyanobacteria	-	0	0	0	0.18	0	-	-	1
Diatoms	-	0.27	0	0	0	0	-	-	1
<i>Winter monsoon</i>									
Dinoflagellates	0.15	0	0	0	0	0	-	-	1
Cryptophytes	0	0	0.23	0	0	0	-	-	1
Chlorophytes	0	0	0.00	0.05	0.02	0.20	-	-	1
Cyanobacteria	0	0	0	0	0.10	0	-	-	1
Diatoms	0	0.17	0	0	0	0	-	-	1

Table 3. Output ratios were estimated with the CHEMTAX programme.

<b>Class/Pigment</b>	<b>Peri</b>	<b>Fuco</b>	<b>Allo</b>	<b>Lut</b>	<b>Zea</b>	<b>Chl b</b>	<b>But</b>	<b>Hex</b>	<b>Chl a</b>
<b>Final Ratio Matrix</b>									
<i>Spring Intermonsoon</i>									
Dinoflagellates	0.22	0	0	0	0	0	0	0	1
Cryptophytes	0	0	0.19	0	0	0	0	0	1
Chlorophytes	0	0	0	0.05	0.01	0.15	0	0	1
Cyanobacteria	0	0	0	0	0.22	0	0	0	1
Diatoms	0	0.18	0	0	0	0	0	0	1
Haptophytes	0	0.05	0	0	0	0	0.05	0.10	1
<i>Summer monsoon</i>									
Cryptophytes	-	0	0.18	0	0	0	-	-	1
Chlorophytes	-	0	0	0.05	0.01	0.17	-	-	1
Cyanobacteria	-	0	0	0	0.21	0	-	-	1
Diatoms	-	0.22	0	0	0	0	-	-	1
<i>Fall Intermonsoon</i>									
Cryptophytes	-	0	0.25	0	0	0	-	-	1
Chlorophytes	-	0	0	0.05	0.02	0.13	-	-	1
Cyanobacteria	-	0	0	0	0.23	0	-	-	1
Diatoms	-	0.15	0	0	0	0	-	-	1
<i>Winter monsoon</i>									
Dinoflagellates	0.20	0	0	0	0	0	-	-	1
Cryptophytes	0	0	0.23	0	0	0	-	-	1
Chlorophytes	0	0	0	0.06	0.02	0.14	-	-	1
Cyanobacteria	0	0	0	0	0.14	0	-	-	1
Diatoms	0	0.22	0	0	0	0	-	-	1

Table 4 Mean concentrations ( $\text{mg m}^{-3}$ ) of photosynthetic carotenoids (PSC), photoprotective carotenoids (PPC), photosynthetic pigments (PSP) and total diagnostic pigments (DP) in the study region.

Season	Site	PPC	PSC	PPC/PSC	PSP	DP
SIM	Coastal.S	$0.16 \pm 0.09$	$0.21 \pm 0.02$	$0.75 \pm 0.36$	$1.50 \pm 0.55$	$0.35 \pm 0.09$
	B	$0.09 \pm 0.05$	$0.21 \pm 0.08$	$0.41 \pm 0.08$	$1.25 \pm 0.53$	$0.31 \pm 0.10$
	Estuary.S	$3.29 \pm 0.58$	$0.12 \pm 0.04$	$30.65 \pm 14.91$	$10.30 \pm 1.82$	$3.46 \pm 0.62$
	B	$2.97 \pm 0.94$	$0.17 \pm 0.05$	$19.24 \pm 10.21$	$10.10 \pm 2.41$	$3.19 \pm 0.88$
SM	Coastal.S	$0.20 \pm 0.11$	$0.18 \pm 0.01$	$1.10 \pm 0.58$	$1.29 \pm 0.05$	$0.29 \pm 0.08$
	B	$0.20 \pm 0.11$	$0.15 \pm 0.01$	$1.34 \pm 0.74$	$1.19 \pm 0.04$	$0.27 \pm 0.08$
	Estuary.S	$1.25 \pm 1.22$	$0.23 \pm 0.18$	$8.41 \pm 9.53$	$5.50 \pm 4.65$	$1.36 \pm 1.11$
	B	$1.44 \pm 1.18$	$0.19 \pm 0.06$	$9.00 \pm 8.68$	$6.48 \pm 4.93$	$1.54 \pm 1.12$
FIM	Coastal.S	$0.15 \pm 0.08$	$0.11 \pm 0.07$	$1.44 \pm 0.16$	$1.16 \pm 0.64$	$0.30 \pm 0.16$
	B	$0.09 \pm 0.06$	$0.09 \pm 0.07$	$1.09 \pm 0.18$	$1.06 \pm 0.65$	$0.23 \pm 0.15$
	Estuary.S	$1.81 \pm 1.34$	$0.16 \pm 0.16$	$16.12 \pm 9.03$	$5.50 \pm 3.11$	$1.97 \pm 1.23$
	B	$1.64 \pm 1.42$	$0.13 \pm 0.11$	$14.42 \pm 7.89$	$5.34 \pm 3.22$	$1.78 \pm 1.36$
WM	Coastal.S	$0.26 \pm 0.14$	$0.49 \pm 0.29$	$0.55 \pm 0.05$	$2.28 \pm 1.33$	$0.62 \pm 0.43$
	B	$0.09 \pm 0.01$	$0.34 \pm 0.00$	$0.27 \pm 0.04$	$1.55 \pm 0.04$	$0.42 \pm 0.05$
	Estuary.S	$1.54 \pm 0.41$	$0.34 \pm 0.16$	$5.82 \pm 3.74$	$4.93 \pm 0.62$	$2.06 \pm 0.41$
	B	$1.08 \pm 0.40$	$0.52 \pm 0.53$	$3.66 \pm 3.19$	$6.05 \pm 2.10$	$1.74 \pm 0.54$

Table 5. Regression coefficient of major environmental parameters and various phytoplankton marker pigments and PFGs (\* significant at 0.05; \*\* significant at 0.01).

Parameters	Salinity	NH <sub>4</sub> -N	NO <sub>3</sub> -N	PO <sub>4</sub> -P	SiO <sub>4</sub> -Si
Chl <i>a</i>	0.001**	0.856	0.340	0.037*	0.001**
Chl <i>c3</i>	0.222	0.215	0.765	0.850	0.051
Chl <i>c2</i>	0.016*	0.081	0.834	0.866	0.022*
Peri	0.284	0.001**	0.206	0.532	0.386
Fuco	0.440	0.031*	0.718	0.434	0.460
Diad	0.084	0.010*	0.466	0.948	0.005**
Allo	0.001**	0.030*	0.052	0.542	0.001**
Diat	0.126	0.625	0.640	0.808	0.001**
Zea	0.143	0.614	0.134	0.008**	0.015*
Lut	0.489	0.045*	0.622	0.212	0.430
Chl <i>b</i>	0.182	0.320	0.334	0.002**	0.011*
Caro	0.097	0.918	0.562	0.021*	0.006**
Dinophytes	0.279	0.001**	0.210	0.538	0.440
Cryptophytes	0.001**	0.028*	0.032*	0.510	0.001**
Chlorophytes	0.005**	0.019*	0.246	0.024*	0.015*
Cyanophytes	0.167	0.286	0.231	0.011*	0.013*
Bacillariophytes	0.582	0.136	0.378	0.733	0.245
Haptophytes	0.385	0.662	0.520	0.727	0.126



Table 6. *p*-value of Student's *t*-test results of the mean of major environmental variables and phytoplankton pigments in the study region ('\*' significant at 0.05; '\*\*' significant at 0.01).

Paired <i>t</i> test (two-tailed) results - <i>p</i> value (between season)						
Parameters	SIM vs. SM	SM vs. FIM	FIM vs. WM	SIM vs. WM	SM vs. WM	SIM vs. FIM
Temp	0.001**	0.001**	0.001**	0.001**	0.001**	0.001**
Sal	0.020*	0.128	0.001**	0.115	0.017*	0.001**
PAR	0.926	0.204	0.289	0.062	0.037*	0.166
Tur	0.003**	0.001**	0.204	0.030**	0.001**	0.008**
pH	0.001**	0.154	0.001**	0.001**	0.001**	0.001**
DO	0.810	0.004**	0.569	0.001**	0.001**	0.001**
Nitrate	0.002**	0.001**	0.031	0.170	0.001**	0.020*
Nitrite	0.533	0.374	0.014*	0.251	0.081	0.750
Ammonium	0.003**	0.001**	0.001**	0.001**	0.001**	0.574
Phosphate	0.001**	0.001**	0.001**	0.022*	0.002**	0.008**
Silicate	0.009**	0.176	0.554	0.012*	0.375	0.086
N/P	0.003**	0.001**	0.527	0.207	0.000**	0.311
Si/N	0.313	0.355	0.002**	0.099	0.009**	0.601
Si/P	0.385	0.003**	0.001**	0.806	0.701	0.001**
Chl <i>a</i>	0.027*	0.689	0.980	0.001**	0.706	0.002**
Chl <i>c3</i>	0.512	0.459	0.156	0.609	0.416	0.139
Chl <i>c2</i>	0.023	0.005**	0.002**	0.001**	0.072	0.759
Peri	0.110	-	0.002**	0.014*	0.002**	0.110
Fuco	0.192	0.230	0.021*	0.016*	0.046*	0.536
Diad	0.043*	0.095	0.001**	0.001**	0.001**	0.516
Allo	0.026*	0.029*	0.094	0.444	0.027*	0.061
Diat	0.200	0.008**	0.009**	0.121	0.566	0.042*
Zea	0.001**	0.072	0.274	0.001**	0.044	0.048*
Lut	0.009**	0.732	0.008**	0.001**	0.002**	0.002**
Chl <i>b</i>	0.001**	0.002**	0.049*	0.007**	0.001**	0.003**
Caro	0.003**	0.469	0.916	0.001**	0.096	0.005**

Table 7. Nutrient stoichiometry (mainly N:P) of major estuaries along the Indian coast

Study Area	Study period	N:P	Reference
Gautami-Godavari Estuary	SWM	6	Tripathy et al.2005
Cochin estuary	Southwest monsoon	39.8 ± 28.2	Madhu et al.2007
	Post monsoon	57.9 ± 33.6	“
	Pre-monsoon	15.9 ± 10.1	“
	September 2007	1.62 - 86	
Godavari estuary	November 2008	20.3 ± 14.3	Sarma et al.2009
Cochin estuary	Post monsoon	6.8 - 262	Madhu et al.2010
	Pre-monsoon	4.8 - 101	“
Kodungallur-Azhikode Estuary	Southwest monsoon	27.9 ± 14.2	Bijoy et al.2014
	Post monsoon	7.4 ± 3.4	“
	Pre-monsoon	4.2 ± 3.6	“
Cochin estuary	Pre-monsoon	6.5- 46.4	Bhavya et al.2016
	Southwest monsoon	2.3 - 24.8	“
	Post monsoon	7.08 - 27.5	“
Kundalika Estuary	Pre monsoon	< 60	Chowdhuri et al.2017
	Southwest monsoon	< 20	“
	Post monsoon	< 25	“
Haldia Estuary	Southwest monsoon	0.6	Bharathi and Sarma 2018
Mahanadi Estuary		1.9	“
Rushikulya Estuary		8.7	“
Krishna Estuary		1.0	“
Ponnayaar Estuary		97.2	“
Zuari Estuary		2.3	“
Mandovi Estuary		0.5	“
Tapti Estuary		0.2	“
Narmada Estuary		23.2	“
Cochin Estuary	Post monsoon	5 ± 3	Jabir et al.2020
	Southwest monsoon	37 ± 15	“
	Pre monsoon	19 ± 9	“